TD 97-001

R54002 Test Report

J. DiMarco, S. Feher, M.J. Lamm, D. Orris, J.P. Ozelis,
J.C. Tompkins, A.V. Zlobin
(FNAL)

February 25, 1997

Contents

List of Figures

List of Tables

Chapter 1

Introduction

Low-β quadrupole R54002 was built from February 1996 to August 1996 and was tested from September 19 to October 11, 1996 at HMTF in IB1 (test stand 5). Testing focused on the following areas (see for detailes Run Plan in Appendix 1).

1. Quench behaviour at 4.3K and 1.8K
2. Quench protection heaters
3. Strain gauge measurements
4. Splice resistance
5. RRR
6. Energy loss measurements

Chapter 2 gives an overview of the magnet and Chapters 3 - 8 present the results of the magnet test.

Chapter 2

Magnet overview

R54002 is a 54" magnetic length "low β quadrupole" (LBQ) built and tested at FNAL. As the name implies, R54002 is the second LBQ magnet built in the post SSC magnet R&D program at Fermilab. The goals for building this magnet were the following:

1. Validate the existing construction techniques for LBQ magnets. The first magnet in this program R54001 was built with existing coils made during the LBQ production manget program. For R54002, new coils were wound and cured from existing LBQ cable.

2. Compare the performance of the magnet at 1.8K to the baseline LBQ magnet with regard to mechanical pretresss in the body and ends.

3. Compare strain gage predictions with ANSYS models [2] during assembly and test.

2.1 Magnet assembly

The magnet design followed the baseline design described in the "Pink Book" [1] and the assembly procedure followed the standard LBQ traveler. Deviations for the baseline design were the following:

1. There are strain transducers in the collars to measure azimuthal coil stresses. The location of the strain gauges are shown on Fig 2.3.

Strain gauge assemblies were placed in the "A" and "C" quadrants, at identical longitudinal positions. Each of the aforementioned quadrants was instrumented with an inner beam gauge and three active pole tip gauges. Additionally, a beam gauge compensator and two pole tip coopensators were placed in each quadrant. The outer beam gauges were placed approximately 32" from the lead end, the three active pole tip gauges were placed approximately 34.5" from the lead end, and the inner beam gauges were placed approximately 35" from the lead end. Compensating gauges were placed about 38" from the lead end. Gauge placement was determined from considerations of coil size data - the "A" and "C" quadrants representing low and high predicted prestresses, respectively.

2. Stainless steel end cans were replaced by aluminum cans; Kapton pole shims were used to increase the body prestress and Kapton radial shims were used to increase the stress in the end region. Table I summarizes the coil sizing and pole shim selection for the body pre-load. The "Calculated Preload" is based on the most up-to-date ANSYS model [2], using a separate spring rate for the inner and outer coil of 0.845 kpsi/mil and 0.665 kpsi/mil respectively. Note that the desired preload is 7.5 kpsi for both inner and outer coils. As shown in chapter 5, there is a significant discerpancy between the calculated preload and the measured preload using strain gauge transducers (see table 5.1) The calculation predicts an inner coil preload lower than measured, while the predicted outer coil preload is significantly higher than measured.

3. The inner coil is instrumented with voltage taps for turns near the pole and the copper wedge. The layout of the voltage taps is summarized in Fig 2.1 and Fig 2.2. The voltage taps were soldered to the coil after removing a tiny piece of the Kapton insulation. The Kapton melts at higher temperatures than the solder so, in principle, the soldering technique should not introduce a turn-to-turn short.

2.2 Repair history

During the assembly of the coil several coil to coil shorts and broken voltage taps were observed and repaired:

1. 4/16/96 Inner coil A had a short; both inner and outer coils were replaced and the magnet was re-collared.

2. 6/25/96 Inner coil D had a short. A metal chip was found between the 2nd and 3rd turn, 13.5" from lead end of the magnet. It was repaired by removing the chip and inserting varnish and Kapton layer. Tha coil was cured over three days and it was pressed with 4720 psi. The Q reading was normal so the magnet was re-assembled (re-collared).

3. 7/29/96 Inner coil D had a short close to voltage tap #11. The cause of the short is very likely related to the broken voltage tap #11. The coil was repaired by partly ($\sim$ 1/3 of the collar from the lead end) un-collaring the coil and inserting Kapton foil at the affected location. The uncollared part of the coil was re-collared.

4. The following voltage taps were repaired: inner coil B voltage tap number 3,4,11 and inner coil D voltage tap number 1,3,14,11,18. All the voltage taps but number 11 on inner coil D were repaired.

Table 2.1: Coil sizes (relative to nominal size), shiming and calculated preloads

Qadrant	Coils #	Coil size [mils]	Added shims [mils]	Total size [mils]	Calc'd preload kpsi
Inner A	101	6.00	5.00	11.00	9.3
Inner B	100	8.25	0.00	8.25	7.0
Inner C	103	7.15	0.00	7.15	6.0
Inner D	102	7.85	0.00	7.85	6.6
Inner Average		7.31		8.56	7.2
Outer A	104	10.00	3.00	13.00	8.6
Outer B	100	11.20	4.00	15.20	10.1
Outer C	102	3.70	5.00	8.70	5.8
Outer D	101	13.20	4.00	17.20	11.4
Outer Average		9.53		13.53	9.0
Inner/outer Average					8.1

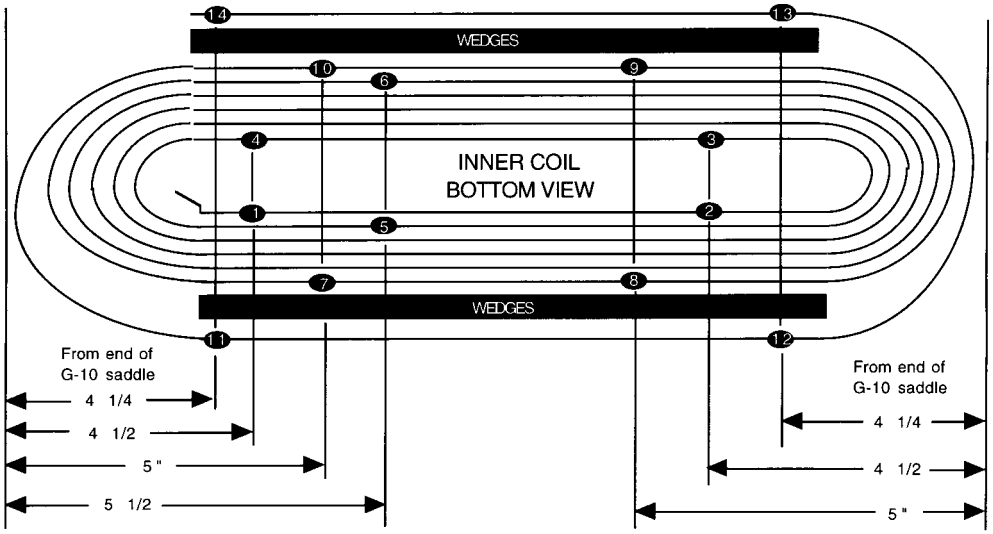

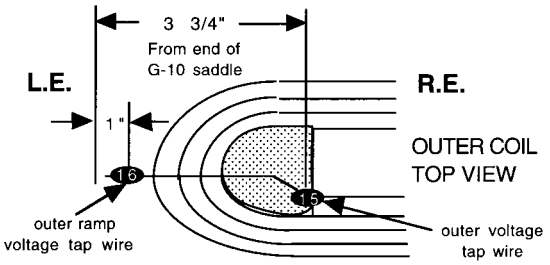

Figure 2.1: Voltage tap location on an inner coil

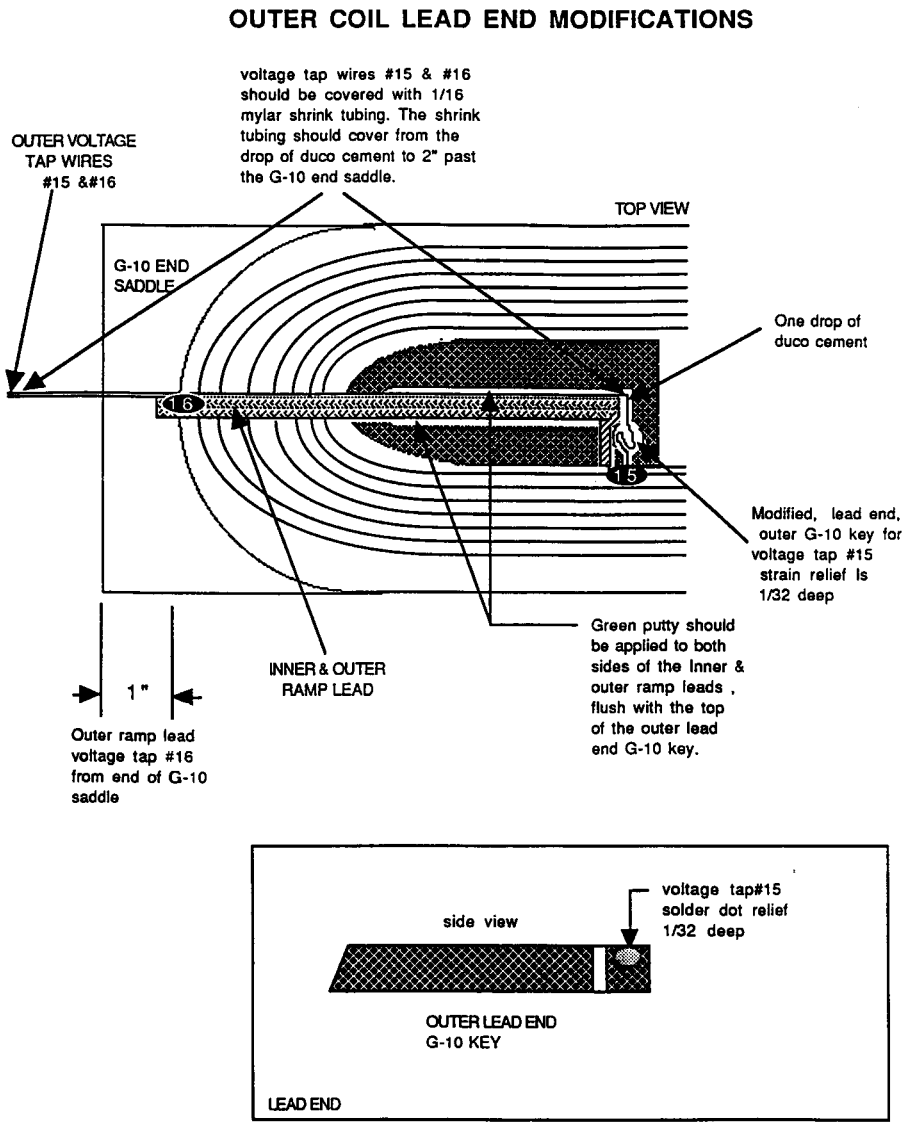

Figure 2.2: Voltage tap locations on the outer coil lead end region

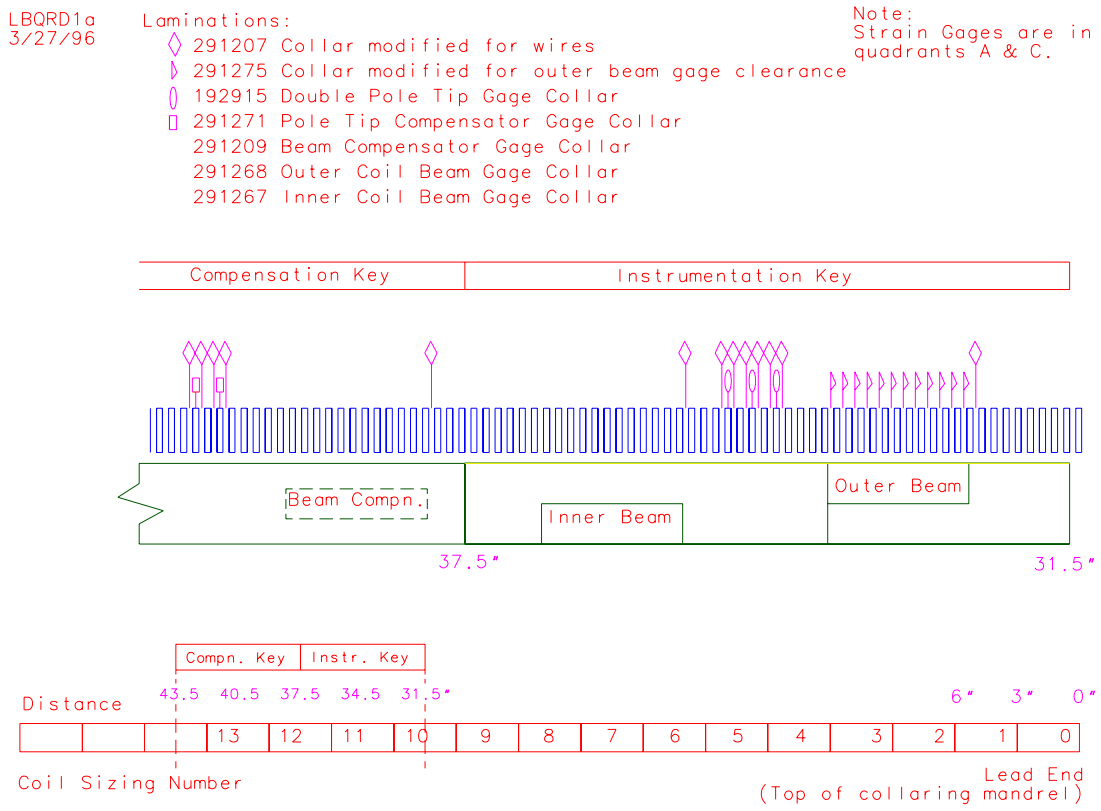

Figure 2.3: Schematic view of the location of the strain gauges

Chapter 3

Quench behaviour

This chapter summarizes the quench behaviour of the magnet. Instrumentation settings for stand 5 are summarized in Table 3.1 and Table 3.2; a detailed description of the instrumentation and its configuration is presented elsewhere [3]. The quench data acquistion was performed using the "SSC" program running on the MDTF01 VAX. The binary quench data were stored on the VAX and later converted to ASCII files for storage on a UNIX workstation. The location of the files on the VAX are: MDTF00::SSC$ROOT:[DATA.QUENCH]R54002.qb*; and on the MTF UNIX cluster: /vmtf/analysis/quench_data/lbqrd2 (see Data File summary in appendix 2). The data were analyzed using the qxplot.sh utility[5]. R54002 had 69 voltage taps, primarily instrumenting the pole turns and wedge on the four inner coil quadrants and inner/outer coil splice regions.

3.1 Spontaneous quench history

R54002 was tested according to the run plan attached as an Appendix to this note. The quench history is summarized in Table 3.3 and in Figure 3.1. Quench testing began at 4.3K at a ramp rate of 16A/s with the first four spontaneous quenches of the magnet occurring at currents of $\sim$ 4.7kA. The predicted short sample limit of the superconducting cable used in this magnet is 5.4kA [4], and so the quench current obtained is far below that expected. However, as all four quenches were at the same location and no clear training was occurring, it was decided to move ahead in the runplan with ramp

rate studies at 4.3K. The magnet was ramped to quench at ramp rates of 32A/s, 300A/s, 200A/s, 150A/s, 100 A/s and 64A/s (quench numbers 5 to 10). In turn, this was followed by cooldown and spontaneous quench testing at 1.8K. The magnet was quenched 10 times (quench numbers 11-20) with an overall, though non-monotonic, increase in current at quench of $\sim$ 500A. As with 4.3K, the current at quench at 1.8K ceased to increase significantly even though it was several hundred Amps below the predicted short sample limit of 7150A[4]. Next, ramps to quench at 1.8K were performed at ramp rates of 300A/s, 200A/s, 150A/s, 100A/s, 75A/s and 50A/s (quench numbers 21-26). After several heater induced quenches, the magnet was again ramped to quench at 16A/s to check whether the quench current would improve. The currents for these quenches were 6369A (quench number 27) and 6107A (quench number 28) - values in the same range as before. After additional 1.8K heater studies, the magnet was warmed to 4.3K and ramped to quench (quench number 29). Since there was no improvement in quench current, we continued with quench current vs. temperature studies in the range 4.3K-1.8K (quench numbers 30-33). The magnet then went through thermal cycle to room temperature (290K).

The second test cycle cooled the magnet down directly to 1.8K and performed quench tests at 16A/s ramp rate (quench numbers 35-37). No improvement in current at quench was observed. After more heater studies at 1.8K and 4.3K, a quench test was performed at 4.3K with lowered cryostat pressure (1.5atm rather than the 4atm normally used) which corresponds to the operating pressure of VMTF (quench number 38). The results of the 1.5atm study would help us in comparing VMTF and HMTF results in the future.

3.2 Quench training

The training curve of R54002 is shown in Fig 3.2. The magnet quench current at 4.3K would seem to be mechanically or otherwise limited since all of the first four quenches were located near the internal splice region of Coil A and the current at quench was less than 4.8kA - several hundred Amps below the expected short sample limit of 5.4kA. The accuracy of localizing the quench using the time of flight technique (see section 4), is not sufficient to

determine whether the quench was located right at the splice or closer to the straight section where the bend of the cable is significant. The 1.8K training curve of the magnet is also shown in Fig3.2. The magnet appeared to train somewhat at 1.8K but the quench current was erratic. Most of the 1.8K quenches were located near the end regions of the magnet though moving unpredictably among the outer and inner A, B, C, and D coils. From Fig3.2 one can conclude that the thermal cycle had no significant effect on spontaneous quench current behavior of the magnet.

3.3 Temperature dependence of quench current

Quench current dependence on temperature is plotted in Fig3.3. Though R54002 quenches did not reach the short sample limit of the superconducting cable, there still was a monotonic decrease in quench current with increasing temperature as expected for a magnet which is not limited by mechanical instabilities. Furthermore, it was observed that below the lambda point there was an additional increase of the quench current relative to what one could expect from the data above the lambda point. This effect is presumably caused by the increased cooling afforded by superfluid He which has higher thermoconductivity and specific heat. The location of the temperature dependence quenches from 2.1K to 4.3K was the inner/outer splice on coil D.

3.4 Quench locations and quench propagation velocity

The 69 voltage taps that instrumented R54002 allowed for localization and determination of propagation velocity for most quenches. The quench propagation velocity was determined using a "time of flight" technique. The basic idea of this technique is to determine the time needed for the quench to propagate between voltage taps separated by a known distance. The start time of a quench in a voltage tap segment was determined by tracing back the voltage rise in the segment to the first point 3σ above the noise. In some cases the end time was determined by the change of the slope of the

voltage growth in the segment where the quench was initiated, rather than the difference between the start times in adjacent segments.

The resulting quench velocity can then be used to determine the location of the quench between the taps. The accuracy of these measurements is on the order of a couple of inches. Fig 3.4 shows the schematic view of the magnet and the location of the voltage taps on the magnet. Figure 3.5 shows the signals collected with voltage taps during a sample spontaneuos quench (quench number 1). The locations of each spontaneous quench and their quench propagation velocities are summarized in Table 3.3. Fig 3.6 is a plot of the quench propagation velocity as a function of quench current. Quench propagation velocity as a function of the normalized current (I/I_c) is plotted in Fig 3.7. From Fig 3.6 and Fig 3.7 one can conclude that the quenches in superfluid helium have quite a different quench propagation velocity than those at 4.3K. This effect might be explained by the better cooling of the cable in superfluid He. Some quenches occurred in locations not well instrumented with voltage taps and could not be well localized (e.g outer coil quenches). Quenches which occurred close to voltage tap number 19 (pole turn of the coil) could be used to measure turn to turn quench propagation velocity using the voltage taps on the next turn. The turn-to-turn quench propagation times as a function of current at quench are shown in Fig 3.8. It would seem that the turn to turn quench propagation velocity does not depend on the cooling condition, but does depend on current at quench.

3.5 Quench current ramp rate dependence studies

R54002 quench current as a function of ramp rate is shown in Fig 3.9. The ramp rate dependence at 4.3K is a steeply falling function and the ramp rate dependence is quite different from another low-β quadrupole R54001[6]. The only explanation is that the magnet is quite sensitive to AC losses, which may be cable contact resistance or splice heating related. The ramp rate dependence at 1.8K is not as steep as it was at 4.3K and it has an additional flat section at lower ramp rates. This might suggest that at lower ramp rates the magnet is limited by other effects than AC losses. It is also interesting to point out that all the higher ramp rate quenches occured in one coil (inner

C).

Table 3.1: Instrumentation settings - spontenaous quenches

Dump Resistor	Resistance	$100m\Omega$
	Time Delay	$100msec$
Power Supply	Time Constant	$0.5sec$
HFU	Capacitance	$14.4mF$
	Time Delay	$30-50msec$
	Voltage	$250V@4.3K$
		$300V@1.8K$
Data Logger	Sampling frequency	$2kHz$
	Pre-quench window	25%
Current read back	Hollec	

Table 3.2: QDC settings

QDC number	Coil gain	Field gain	Balance	Treshold
1	1.	1.0	10.00	0.25
2	1.	10.0	0.72	0.05
3	1.	10.0	0.04	0.25
4	1.	0.1	0.00	1.10
6	1.	1.0	0.05	0.30
7	1.	0.1	0.00	0.10

Table 3.3: Quench history

Quench num	I_q [A]	T [K]	dI/dt [A/s]	Quenched Coil	Quench location	Q_vel [m/s]	Turn-turn time [ms]	File num
1	4694.1	4.3	16	innerA	Vtap19a	89	16	qb005
2	4767.5	4.3	16	innerA	Vtap19a	89	17	qb006
3	4811.5	4.3	16	innerA	Vtap19a	73	17	qb007
4	4748.0	4.3	16	innerA	Vtap19a	89	17	qb008
5	4782.2	4.3	32	innerD	Vtap19b	73	17	qb009
6	2634.9	4.3	300	innerC	Vtap19a	6	58	qb010
7	3525.1	4.3	200	innerC	Vtap19a	21	33	qb011
8	4019.1	4.3	150	innerC	Vtap19a	40	25	qb012
9	4513.5	4.3	100	innerC	Vtap19a	60	20	qb013
10	4684.4	4.3	64	innerC	Vtap19a	73	17	qb014
11	5711.5	1.8	16	innerB	le.st.19bd	39	11	qb017
12	5955.1	1.8	16	outerD	rt.	46		qb018
13	5638.2	1.8	16	innerA	rt.st.19bd			qb019
14	6025.6	1.8	16	outerC	rt.	36		qb020
15	5965.9	1.8	16	outerC	rt.	36		qb021
16	5408.3	1.8	16	innerC	rt.st.19bd			qb022
17	6127.3	1.8	16	outerB	rt.	35		qb023
18	6200.7	1.8	16	innerA	rt.	48		qb025
19	6083.3	1.8	16	innerD	md.st.sec			qb026
20	6264.3	1.8	16	innerA	rt.	45		qb030
21	5158.8	1.8	300	innerC	Vtap19a	28		qb031
22	6005.0	1.8	200	innerC	Vtap19a	39		qb032
23	5995.2	1.8	150	innerC	Vtap19a	52		qb033
24	6137.1	1.8	100	outerC	rt.	50		qb034
25	6220.3	1.8	75	outerC	rt.	50		qb035
26	6293.6	1.8	50	outerD	le.	52		qb036
27	6269.2	1.8	16	innerA	rt.	40		qb047
28	6107.7	1.8	16	innerA	rt.	40		qb048
29	4801.8	4.3	16	innerD	Vtap19b	70	18	qb058
30	5119.7	3.6	16	innerD	Vtap19b	66	17	qb070
31	5369.2	3.1	16	innerD	Vtap19b	66	16	qb071
32	5515.9	2.7	16	innerD	Vtap19b	63	16	qb073
33	5701.8	2.1	16	innerD	Vtap19b	57	14	qb074
34	5990.4	1.8	16	innerC	rt.	37		qb079
35	6269.2	1.8	16	outerA				qb080
36	6093.1	1.8	16	innerA	le.st.19db	48		qb081
37	6058.8	1.9	16	innerA	rt.	48		qb086
38	4855.6	4.3	16	innerD	Vtap19b	78	21	qb093

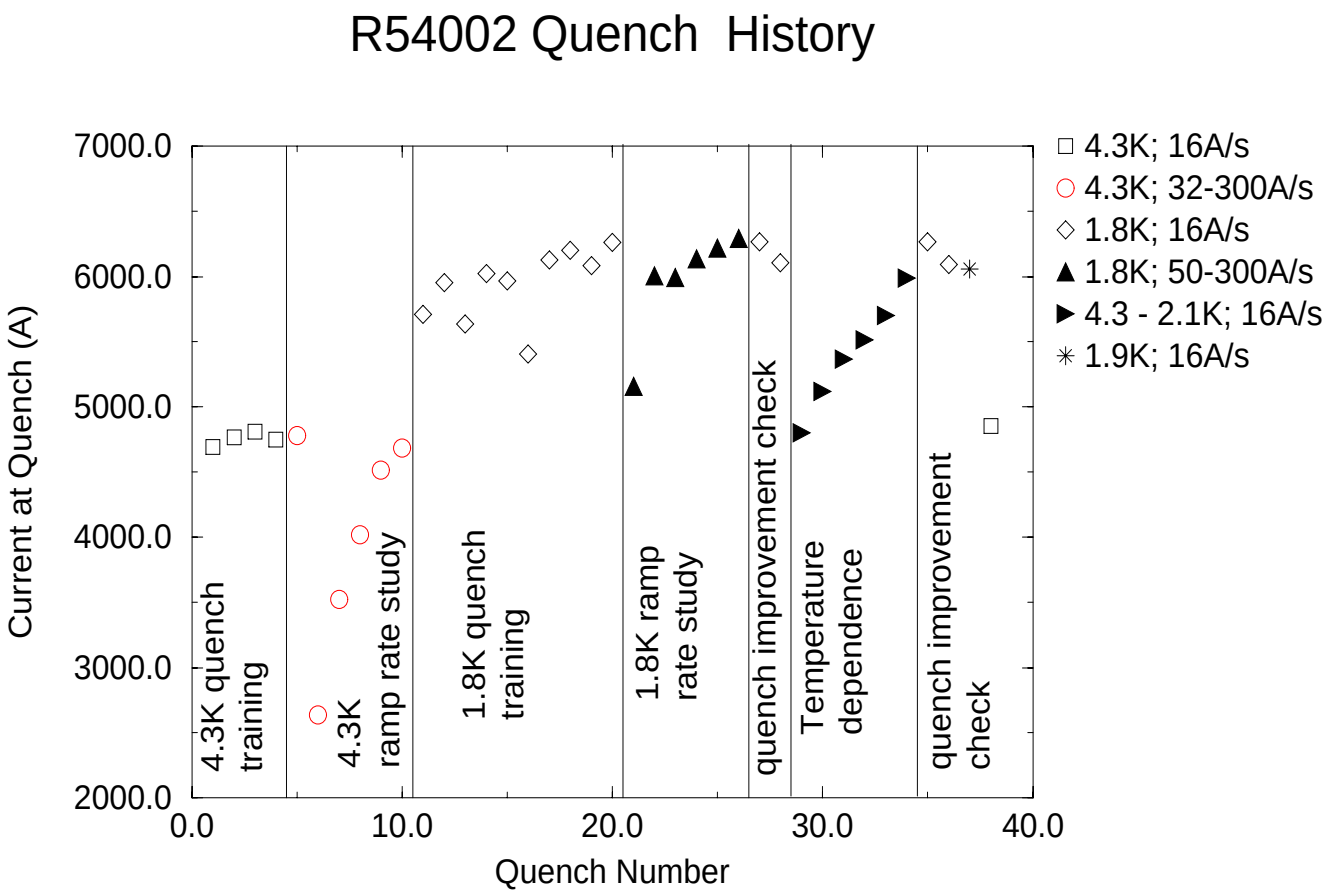

Figure 3.1: Quench history

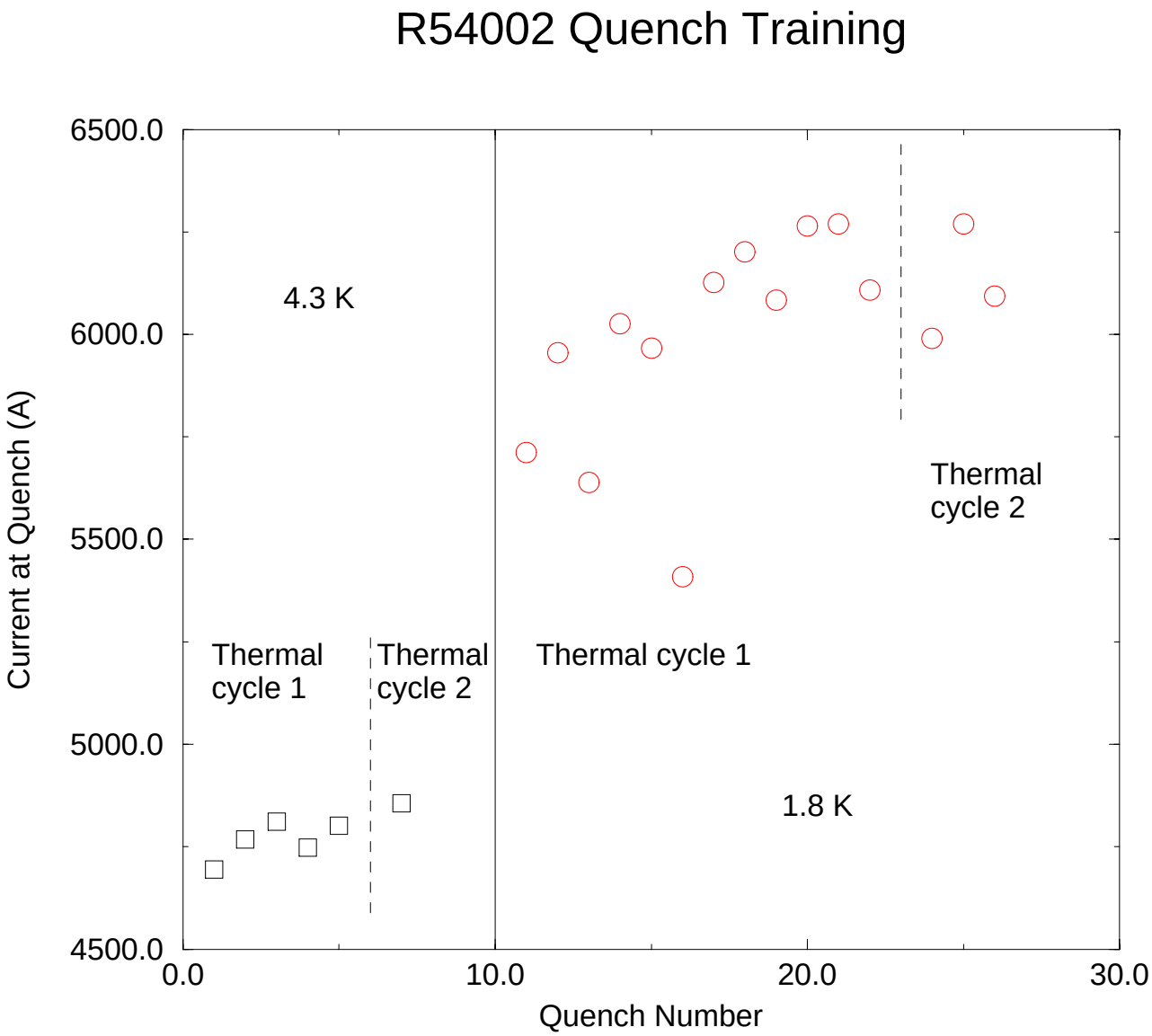

Figure 3.2: Training quenches

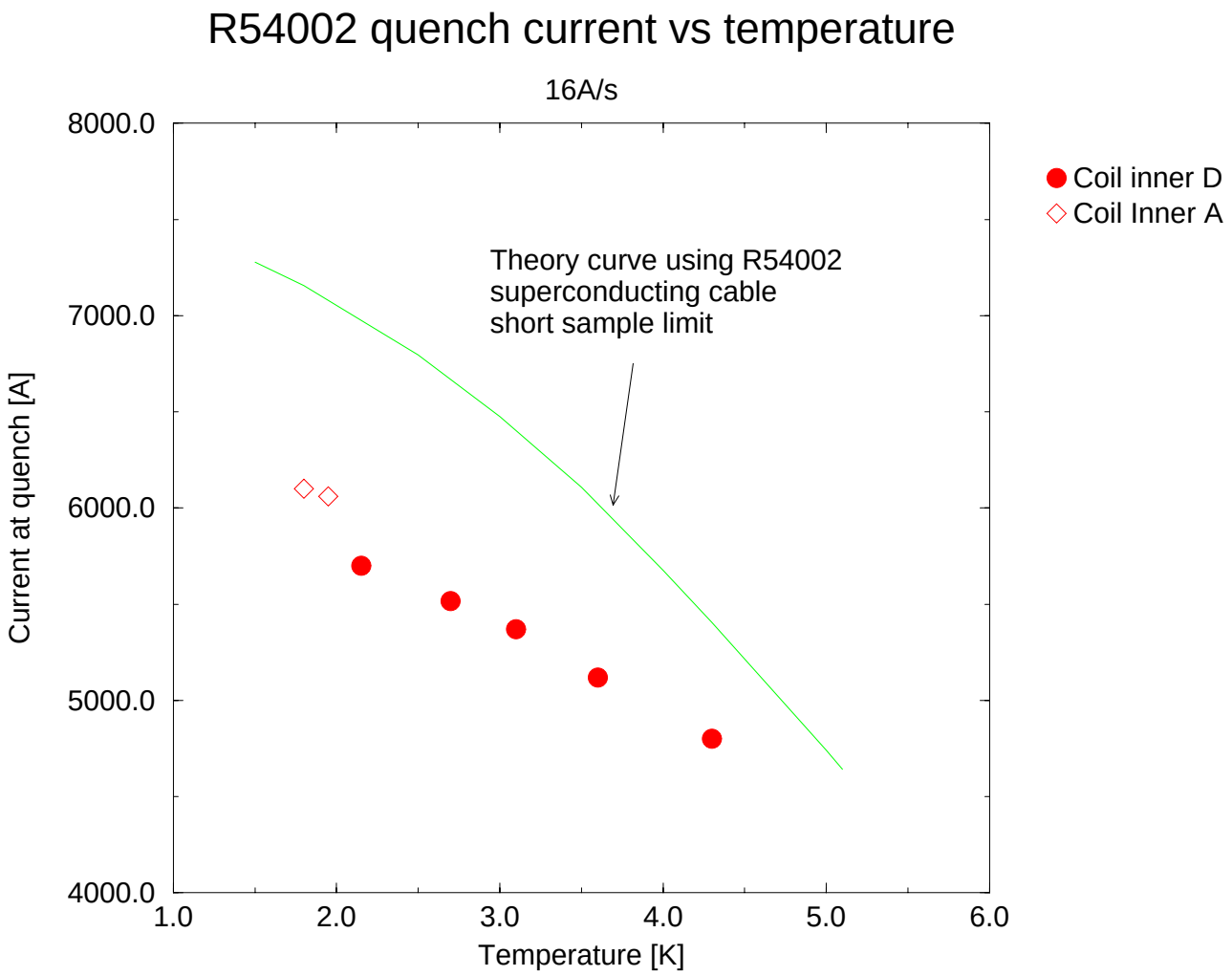

Figure 3.3: Quench current temperature dependence

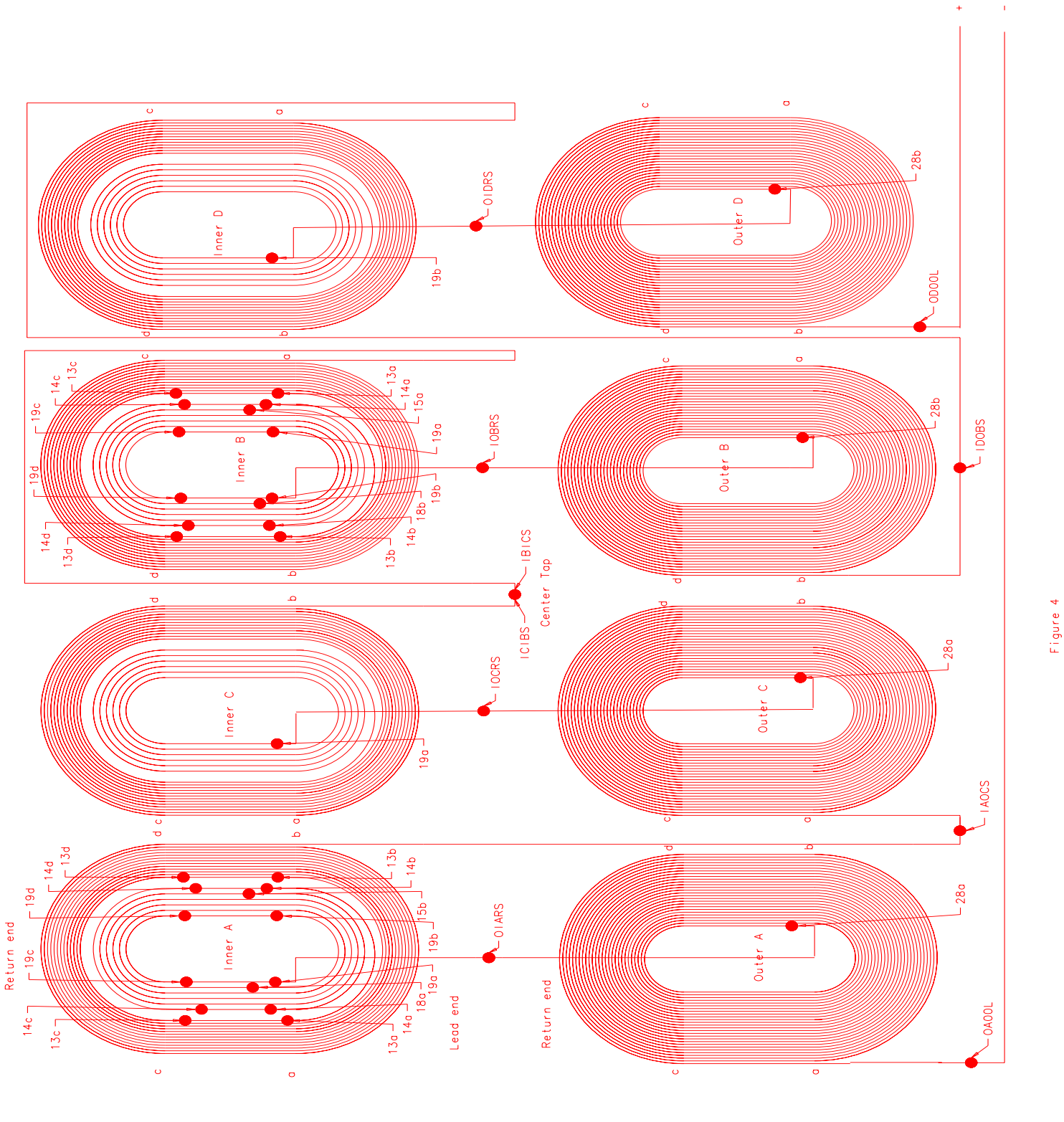

Figure 3.4: Layout of the coils and location of the voltage taps

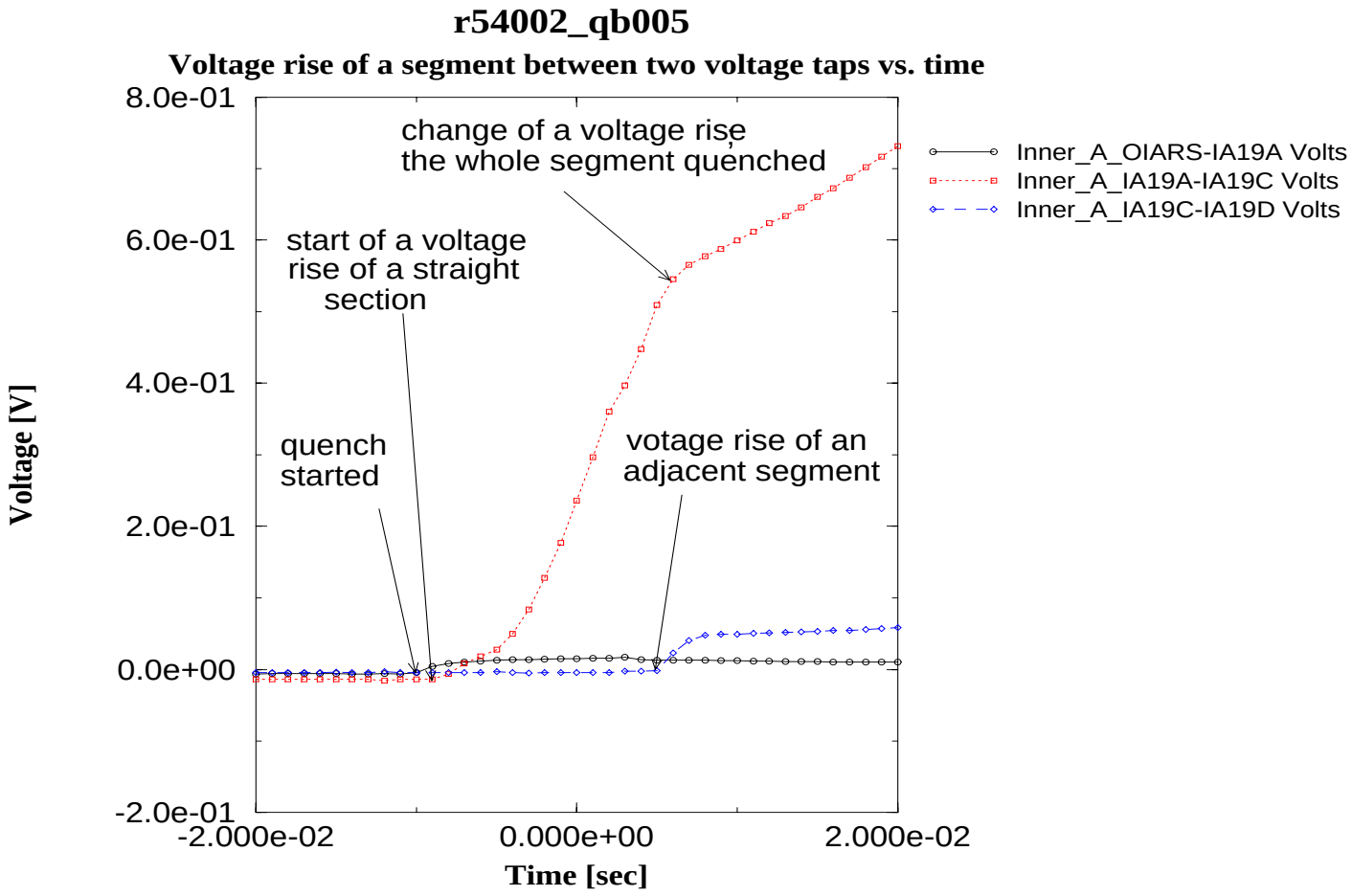

Figure 3.5: Voltage rise

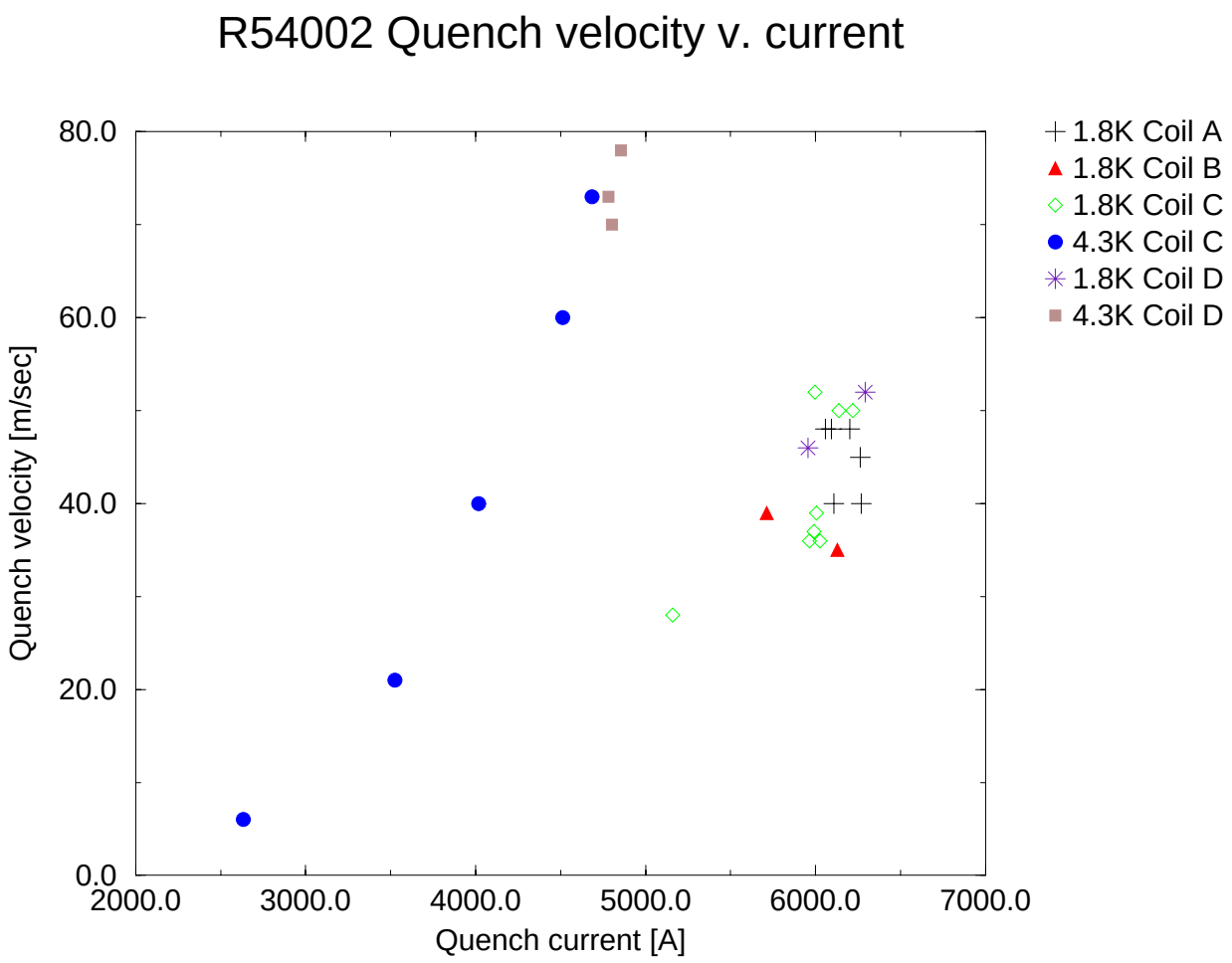

Figure 3.6: Quench propagation velocity as a function of the current at quench

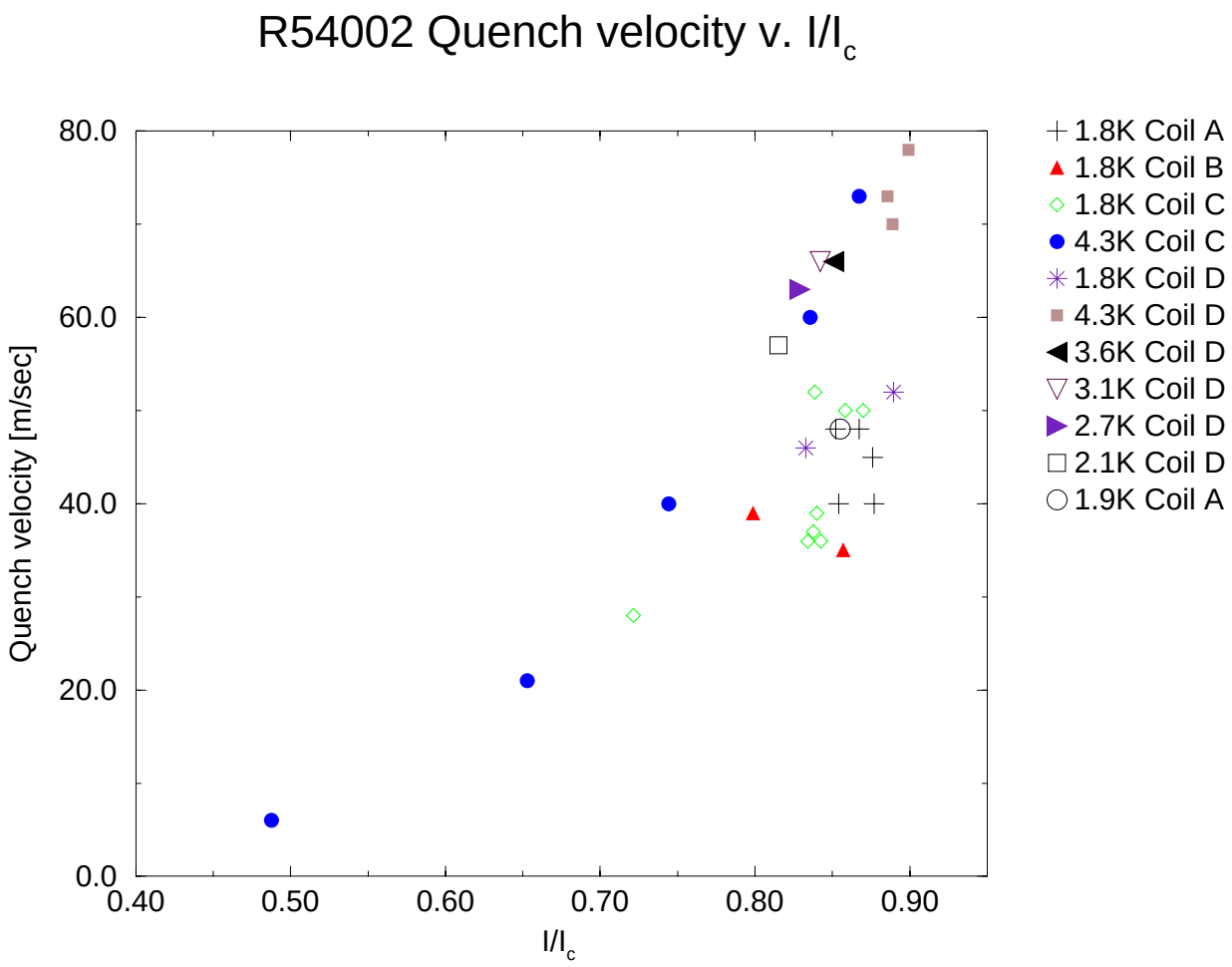

Figure 3.7: Quench propagation velocity as a function of I/I_c

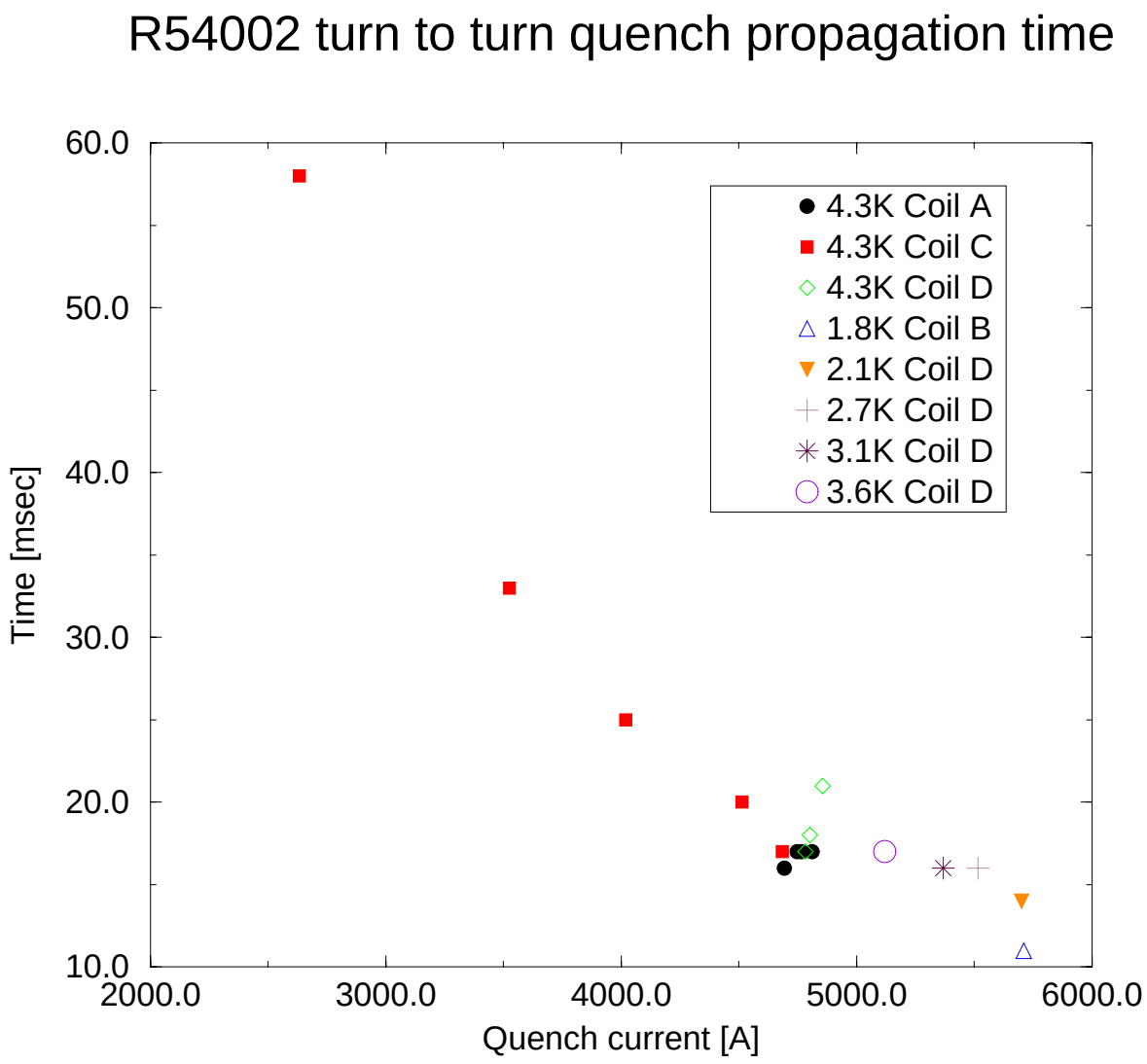

Figure 3.8: Quench turn-to-turn propagation time as a function of the current at quench

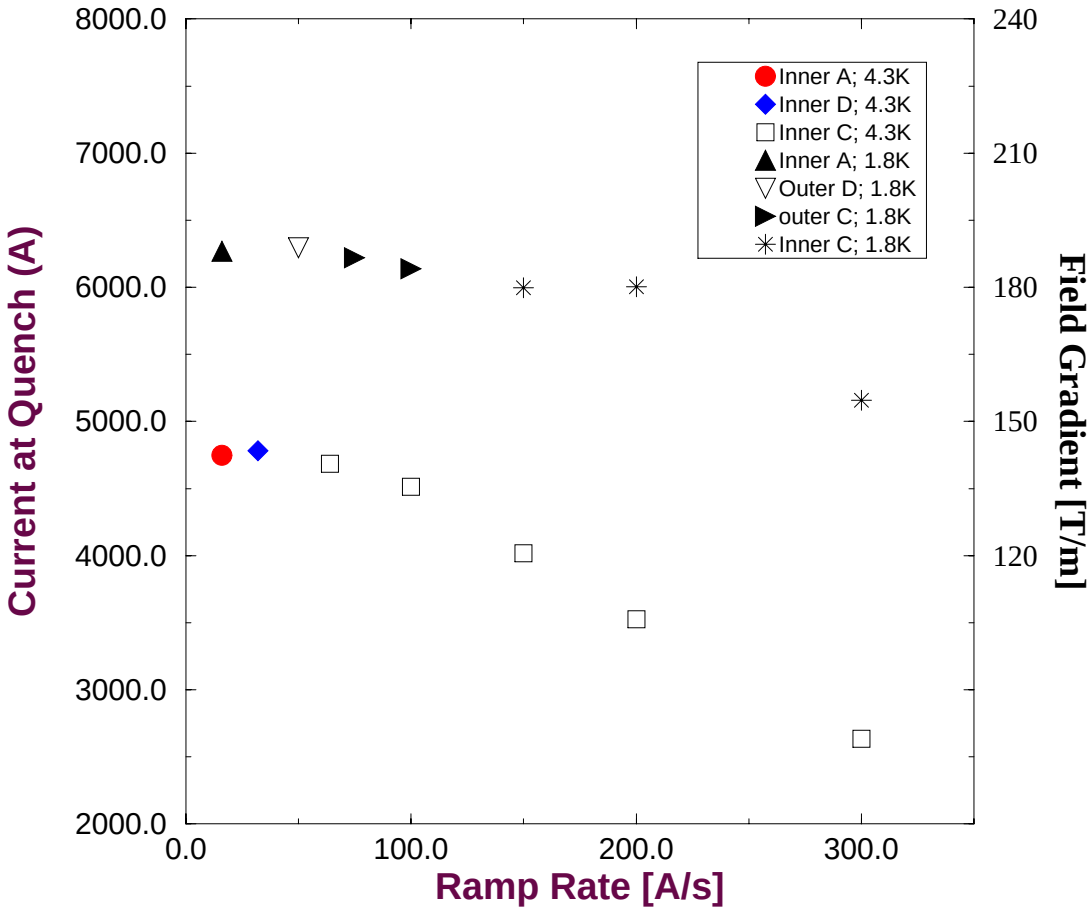

Figure 3.9: Quench current ramp rate dependence

Chapter 4

Quench protection heater study

This chapter presents the results of the quench protection heater studies. The overview of the magnet is described in chapter 2, and a detailed description of the instrumentation and its configuration presented in [3]. R54002 had 69 voltage taps, primarily instrumenting the pole turns and wedge on the four inner coil quadrants and inner/outer coil splice regions. Instrumentation and heater firing unit parameters for stand 5 are summarized in Table 4.1 and Table 4.2.

The quench data acquistion was performed using the "SSC" program running on the MDTF01 VAX. The binary quench data were stored on the VAX and later converted to ASCII files for storage on a UNIX workstation. The location of the files on the VAX are: MDTF00::SSC$ROOT:[DATA.QUENCH]R54002.qb*; and on the MTF UNIX cluster: /vmtf/analysis/quench_data/lbqrd2 (see Data File summary in appendix B). The data were analyzed using the qxplot.sh utility[5].

4.1 Low-β quadrupole heaters

A schematic of the heater location with respect to the coil is shown in Fig 4.1. The heaters are 25μm thick and 12.5 mm wide stainless steel strips and are located radially beyond the outer coil, in the middle of four layers of 125 μm Kapton sheets. One heater covers approximately 12 turns of two

midplane-adjacent outer coils. This is accomplished by running the heater longitudinally along the body of the magnet and making appropriate folds on the heater in the magnet return end region. Two heaters oriented 180 degrees apart provide coverage for one side of each of the four outer coils. The resistance of the heater for coils A and B was 5.5 Ω, and that for C and D was 5.0 Ω. The system resistance (including cabling from the Strip Heater Firing Unit (SHFU) to the magnet) was 3.0 Ω , which means that $\sim$ 85.5 % of the SHFU voltage was deposited directly to the heaters. Note that in all studies, the voltage reading of the SHFU is used as the voltage applied to the heater.

4.2 Heater induced quenches

In the heater studies, the minimum energy required to initiate a quench as well as the time delay, t_{fn} (the time from protection heater current initiation to the presence of a detectable quench voltage in the outer coils), were measured as a function of various heater, heater power supply, and magnet parameters. The minimum voltage to induce a quench (V_{min}) was determined by firing the SHFU at a voltage low enough not to initiate a quench and then gradually increasing the SHFU voltage and re-firing until the magnet did quench. Since the last voltage set on the SHFU that first initiated a quench was taken as V_{min} and the voltage increments were 10 volts, the uncertainty of the determination of the minimum voltage is $\sim$ 10V. Fig 4.2 shows an example of the t_{fn} determination. Both the start time of the quench and the time of the heater firing were given by the SSC program. Since the SSC program uses the signal provided by the QDC circuit, there can in principle be an error in the determination of the quench start time if the bucked signals tend to compensate each other. The quenches were each checked and if necessary corrected for these ambiguities.

The results are summarized in Table 4.3 and in Figures 4.3 to 4.7 . The I_c used in the plots (for current normalization) correspond to the expected short sample limit of the superconducting cable: 5400A @ 4.3K and 7150A @ 1.8K[4].

4.2.1 Minimum quench voltage

Fig 4.3 shows the minimum SHFU voltage required to quench the magnet as a function of the magnet current at quench. As expected, the deposited energy increases as the applied current decreases and one is further from the critical surface. Furthermore, one can conclude that by setting the SHFU voltage to 300V, the heaters can always initiate a quench in the outer coils for magnet currents greater than 1500A. Fig 4.4 shows the same data as Fig 4.3 except with normalized current I/I_c (where I is the magnet current at quench and I_c is the expected short sample limit of the superconducting cable). The two curves (4.3K and 1.8K) overlay very well, indicating that it is the peak power which determines the energy deposited into the cable. The deviation of the 4.3K curve from the expected shape at low I/I_c values reflects the fact that the peak power is no longer the only variable which matters and that other parameters (e.g. the *total* deposited energy) are involved.

4.2.2 Time delay t_{fn}

Fig 4.5 shows t_{fn} as a function of the square of the SHFU voltage for four different cases of magnet current and the Helium bath temperature. As one can see, at the lower heater energies (close to V_{min}) the t_{fn} increases rapidly while at higher energies t_{fn} levels off. At sufficiently large SHFU voltage, t_{fn} does not change significantly with changes in SHFU voltage.

In Fig 4.6 t_{fn} was plotted as a function of I/I_c at a fixed (and relatively high) SHFU voltage. It shows a definite decrease of the t_{fn} as I/I_c increases.

In Fig 4.7 we plotted t_{fn} for each of the four coils in contact with the heaters as a function of the square of the SHFU voltage. These data are at 1.8K He bath temperature and 1500A magnet current. At low SHFU voltages, the coils show quite a large spread in their t_{fn} values, it could be indicative of small differences in the magnet construction favoring the quenching of some coils over others. At larger SHFU voltages this spread decreases and all four coils quench with similar t_{fn}. Therefore to avoid an unreasonably large spread of the individual coil t_{fn} values, the SHFU voltage should be set sufficiently high with respect to the coil which has the largest t_{fn}.

Table 4.1: Instrumentation settings - heater induced quenches

Dump Resistor	Resistance	$100m\Omega$
	Time Delay	$20 - 30msec$
Power Supply	Time Constant	$0.5sec$
SHFU	Capacitance	$14.4mF$
	Voltage	$197 - 400V@4.3K$
		$86 - 400V@1.8K$
Data Logger	Sampling frequency	$1kHz$
	Pre-quench window	50%
Current read back	Hollec	

Table 4.2: QDC settings

QDC number	Coil gain	Field gain	Balance	Treshold
1	1.	1.0	10.00	0.25
2	1.	10.0	0.72	0.05
3	1.	10.0	0.04	0.25
4	1.	0.1	0.00	1.10
6	1.	1.0	0.05	0.30
7	1.	0.1	0.00	0.10

Table 4.3: Heater induced quenches

I_q [A]	T [K]	SHFU Voltage [V]	t_{fn} [ms] coil A	t_{fn} [ms] Coil B	t_{fn} [ms] Coil C	t_{fn} [ms] Coil D	File num
1485.4	4.3	225	213				qb003
1485.4	1.8	275			213		qb015
1495	1.8	268			308		qb037
1495.2	1.8	295	177	228	152	177	qb038
1495.2	1.8	318	138	162	128	138	qb039
1495.2	1.8	339	122	132	112	122	qb040
1495.2	1.8	360	117	122	107	117	qb041
1495.2	1.8	379	102	107	97	102	qb042
2996.8	1.8	200		88			qb043
2992.0	1.8	197		97			qb044
2992.0	1.8	241		78	83		qb045
5188.2	1.8	110			78		qb046
5990.0	1.8	91			82	78	qb049
5990.4	1.8	120			52	48	qb050
5990.4	1.8	147			48	44	qb051
5990.4	1.8	190		57	42	38	qb052
5990.4	1.8	225		41	39	35	qb053
5990.4	1.8	252		39	37	33	qb054
5188.2	1.8	291		40	38	34	qb055
5188.2	1.8	191		52	50	40	qb056
6190.9	1.8	86				90	qb057
996.3	4.3	237			345		qb059
996.3	4.3	290			117		qb060
1001.2	4.3	335	101	111	95	101	qb061
996.3	4.3	376	88	99	83	89	qb062
2297.4	4.3	201			105		qb063
3794.1	4.3	125		79			qb064
4493.6	4.3	100			75		qb065
4493.6	4.3	141		54	52		qb066
4493.6	4.3	173		47	45		qb067
4493.6	4.3	223			42	42	qb068
4488.7	4.3	283			37	37	qb069
5985.0	1.8	399	37	49	29	29	qb082
1485.4	1.8	400	115	105	112	105	qb083
5990.4	1.8	338	57	31	31	31	qb085
986.5	4.3	400	80	90	80	80	qb089
1236.0	4.3	232			368		qb090
1886.5	4.3	225			196		qb091
4488.7	4.3	401	42	39	31	31	qb092
986.5	4.3	230			302		qb094
1485.4	4.3	220			261		qb095
4488.7	4.3	105			66		qb096

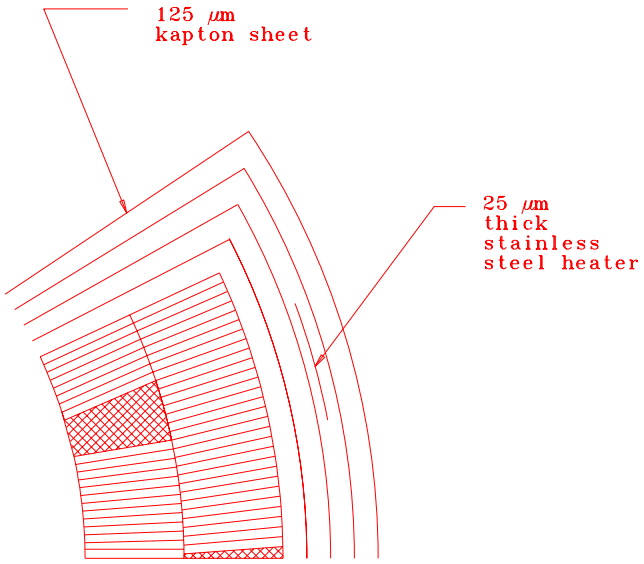

Figure 4.1: Schematic view of the location of the quench protection heater

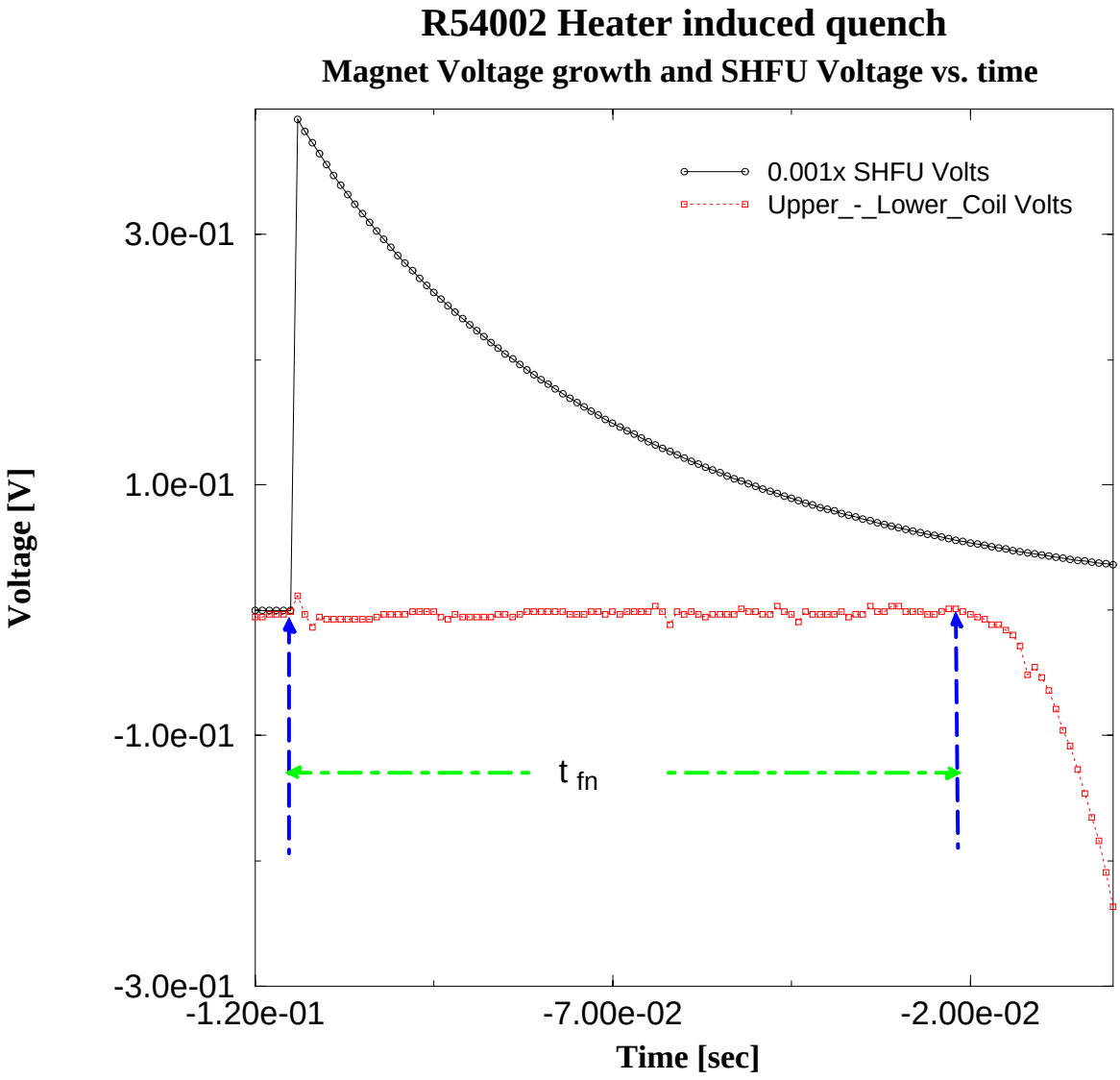

Figure 4.2: Description of t_{fn}

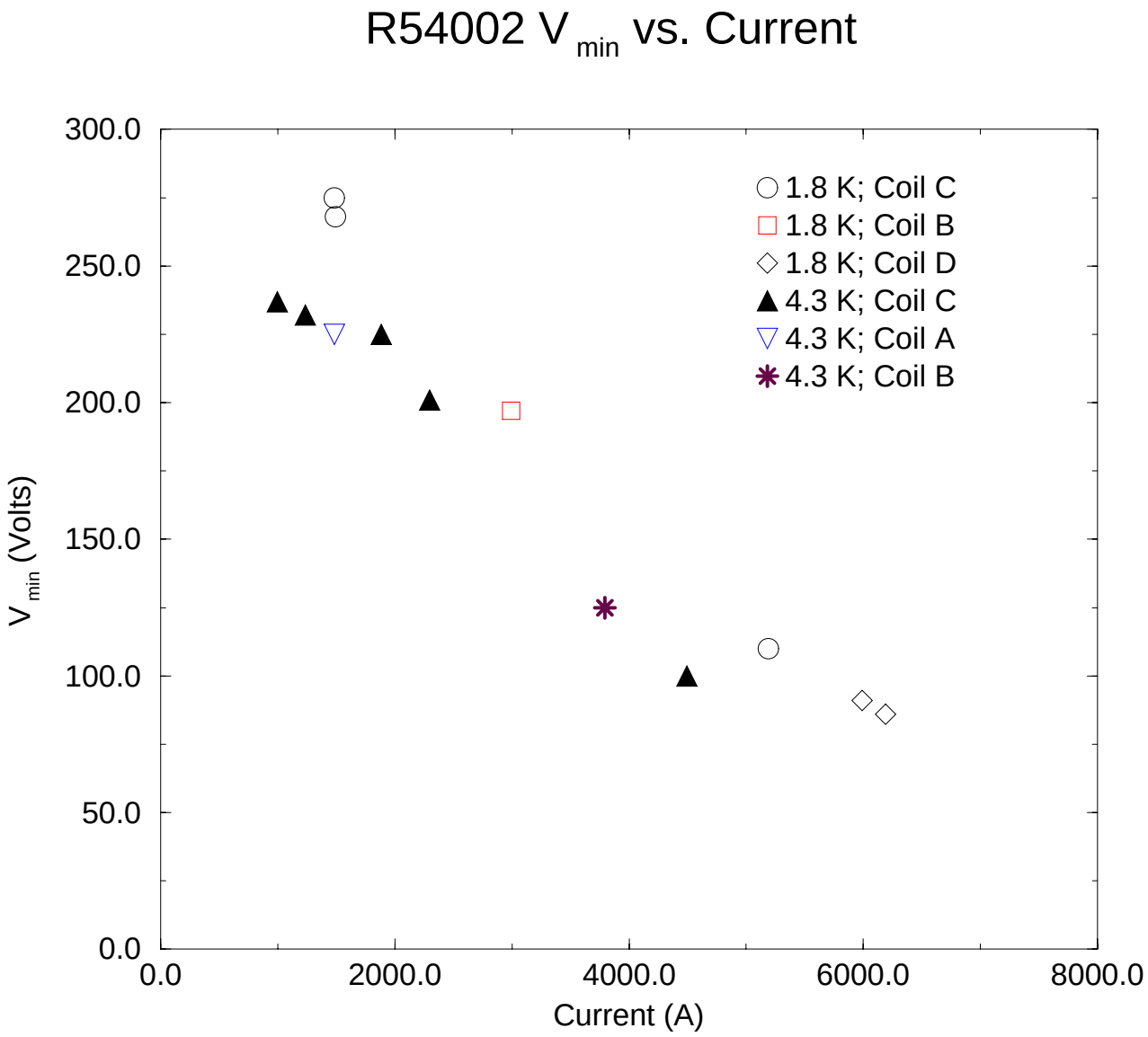

Figure 4.3: Heater induced quenches. Minimum heater voltage to quench the magnet vs. current at quench

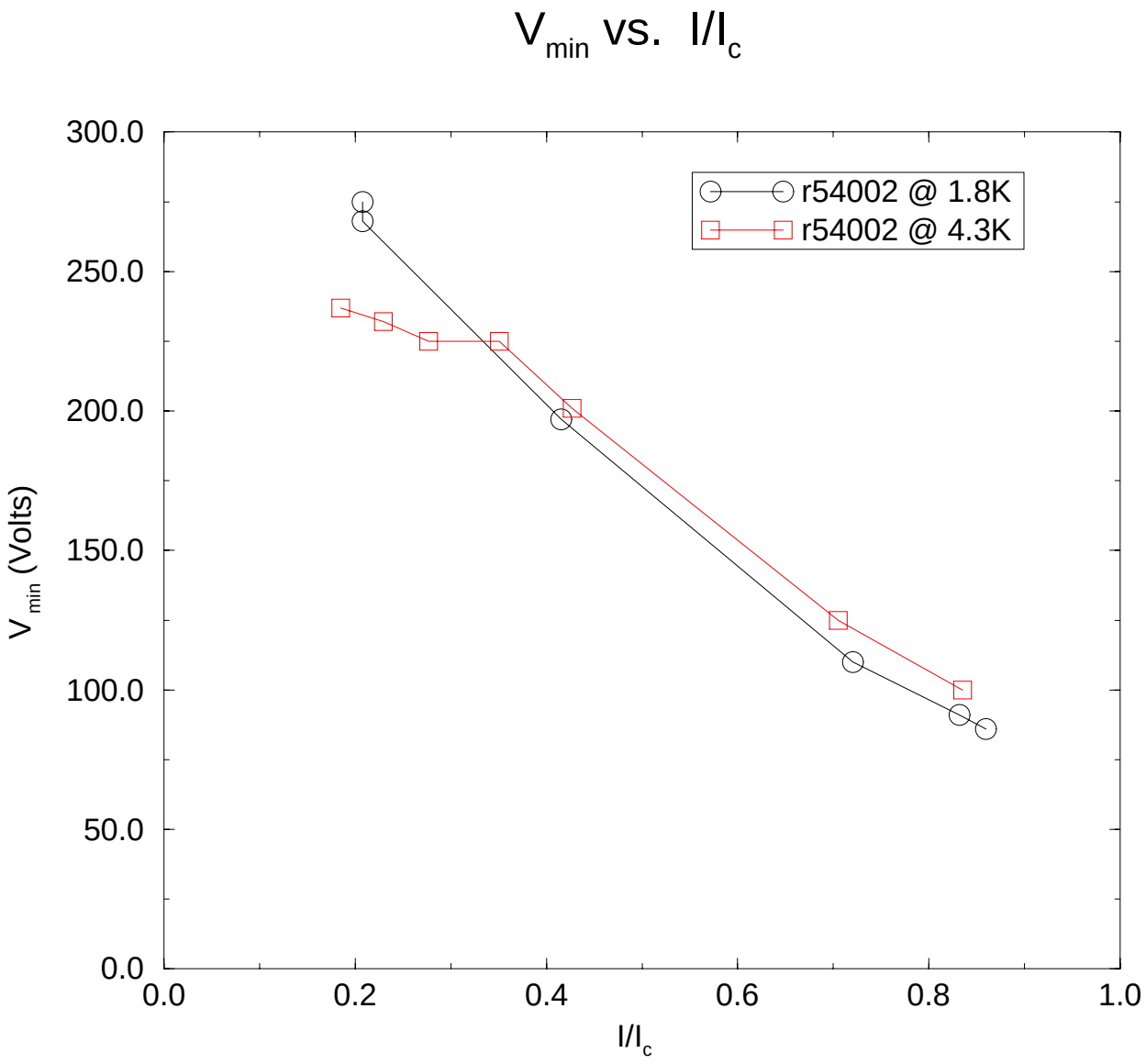

Figure 4.4: Heater induced quenches. Minimum heater voltage to quench the magnet vs. normalized current at quench

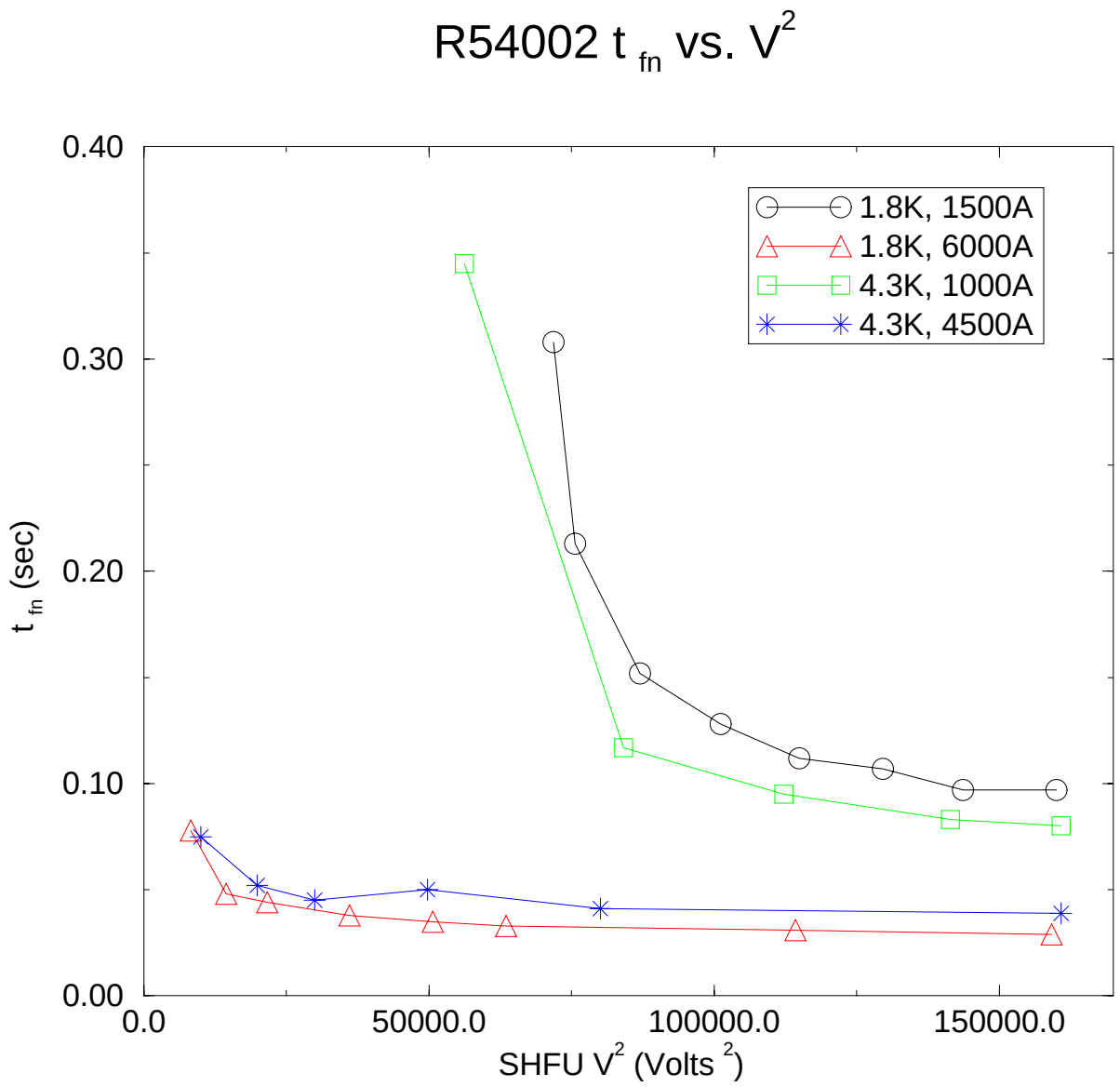

Figure 4.5: t_{fn} vs. square of the heater voltage

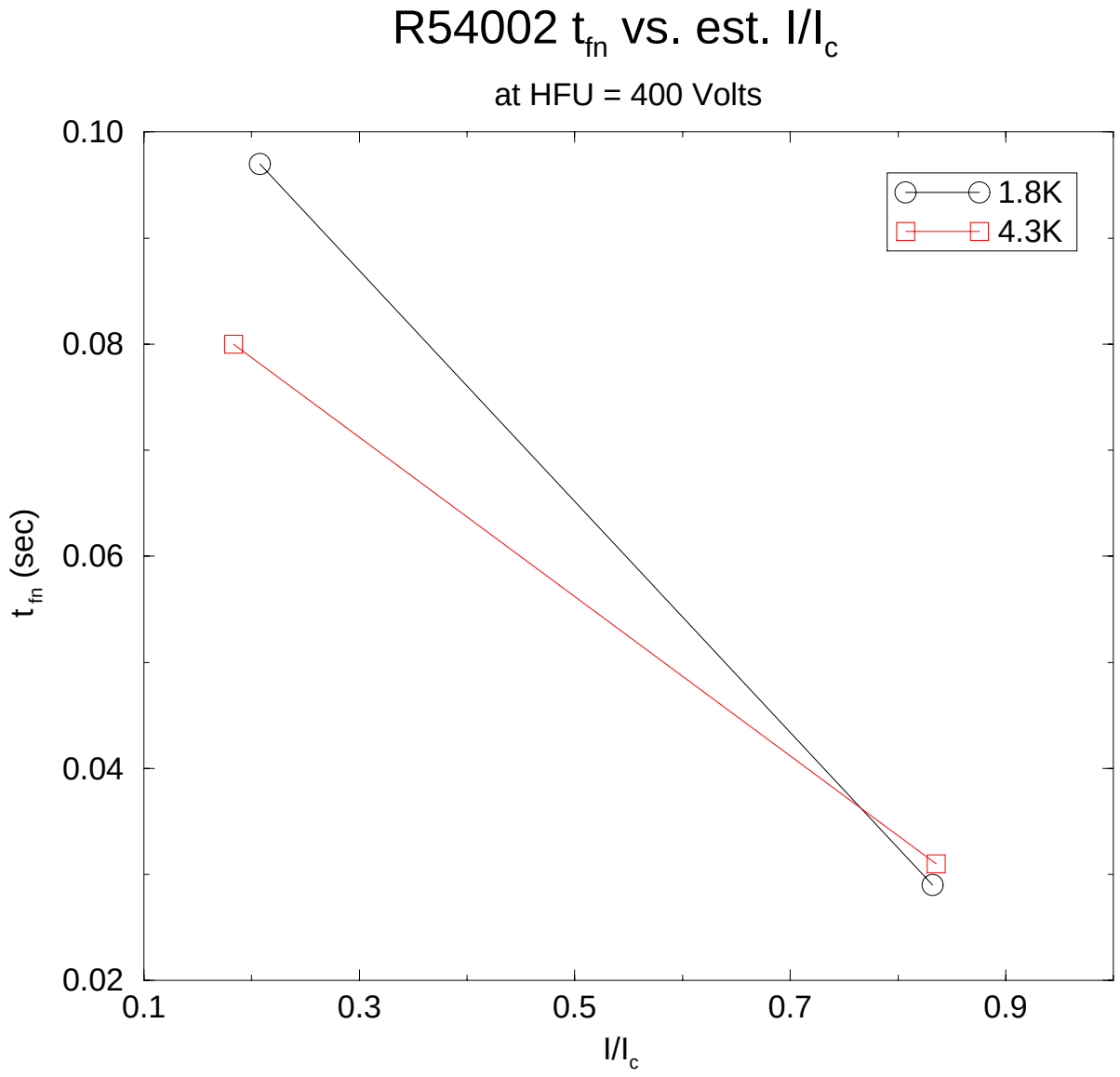

Figure 4.6: t_{fn} is plotted as a function of I/I_c at a fixed (and relatively high) SHFU voltage

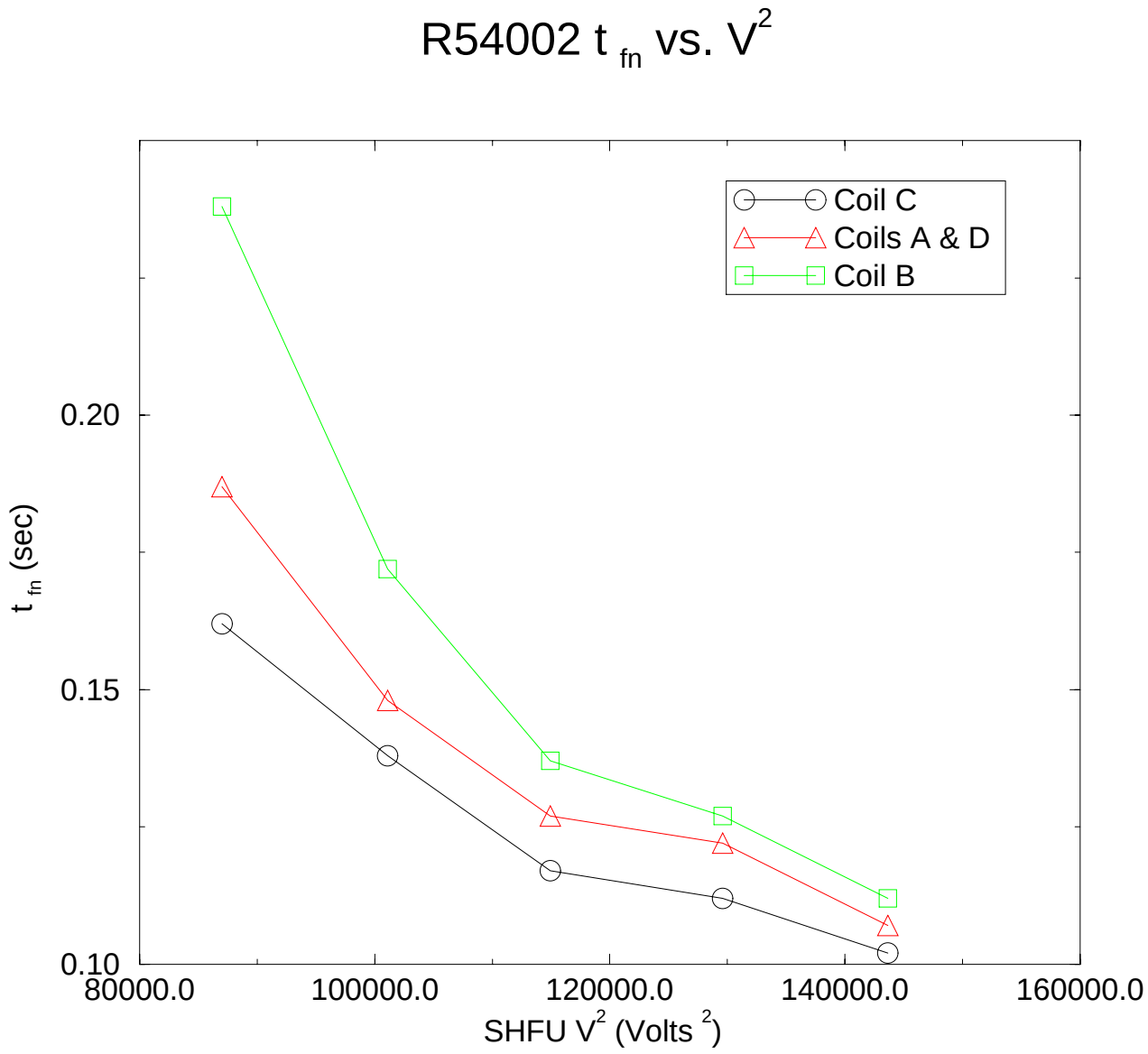

Figure 4.7: t_{fn} is plotted for each of the four coils in contact with the heaters as a function of the square of the SHFU voltage.

Chapter 5

Strain gauge measurement results

Strain gauges to measure coil stresses were installed in magnet R54002 (for more details see chapter 2). Strain gauge runs were perfomed at both 4.35 and 1.8 K, following the run plan. Fig 5.2 shows the coil stresses as recorded by the inner and outer beam gauges as a function of increasing current at 1.8K, for one of these runs. The coil stresses are plotted against the square of the magnet current, yielding a linear dependence, as expected from the nature of the Lorentz forces acting on the conductor. There does not appear to be evidence of complete coil unloading. In Table 5.1 (Fig 5.1) we summarize the inner and outer coil stresses at various magnet conditions/temperatures.

The coil pre-stress gain between collaring and yoking is about 3000 psi for the inner coils and about 1800 psi for the outer coils. A coil stress relaxation of about 5% occurs during the interval between yoking and testing. Upon cooldown to 4.3K, the inner coil pre-stress decreases about 2000 psi, while the outer coil pre-stress loss is about 1500-3000 psi. This would indicate that collar-yoke contact has decreased upon cooldown, as measured coil stress at this stage is systematically lower than that for the collared coil alone. Upon excitation to operating current at 4.3K, we find that the outer coil stresses have decreased to about 1000-1500 psi, while substantial pre-stress (4500-5000 psi) still remains on the inner coils. At 1.8K and I=0, we find essentially the same level of coil stresses as at 4.3K and I=0, though there is a slight systematic decrease of a few to several hundred psi. At excitation to 6000A, we find that the inner coil pre-stresses decreases to about 3000

psi, while the outer coils are essentially unloaded, with pre-stresses less than 1000psi.

Cold calibrated pole-tip gauges were also included in quadrant "A" of this magnet. It has been found through mechanical model studies that pole tip gauge calibrations may not be valid for cases where only the inner (outer) coil carries significantly more stress than the outer (inner) [7]. For this reason, we do not present results from these gauges during cold testing.

Table 5.1: Measured Coil Stresses During Construction and Testing (in psi)

Gauge	Collaring 8/3/96	Yoking 8/8/96	MTF - 300K 9/17/96	4.3K $I = 0$ 9/20/96	4.3K $I \sim I_q$ 9/20/96	4.3K $I = 0$ 9/20/96	1.8K $I = 0$ 9/22/96	1.8K $I \sim I_q$ 9/22/96
BGIA	8961	12814	11065	8960	5318	8045	8093	3393
BGOA	2500	4302	3360	1811	922	1941	1723	602
BGIC	8500	11826	9945	7950	4412	7665	7565	2457
BGOC	4750	6696	5800	2801	1629	2660	2517	894

Figure 5.1: Measured Coil Stresses During Construction and Testing (in psi)

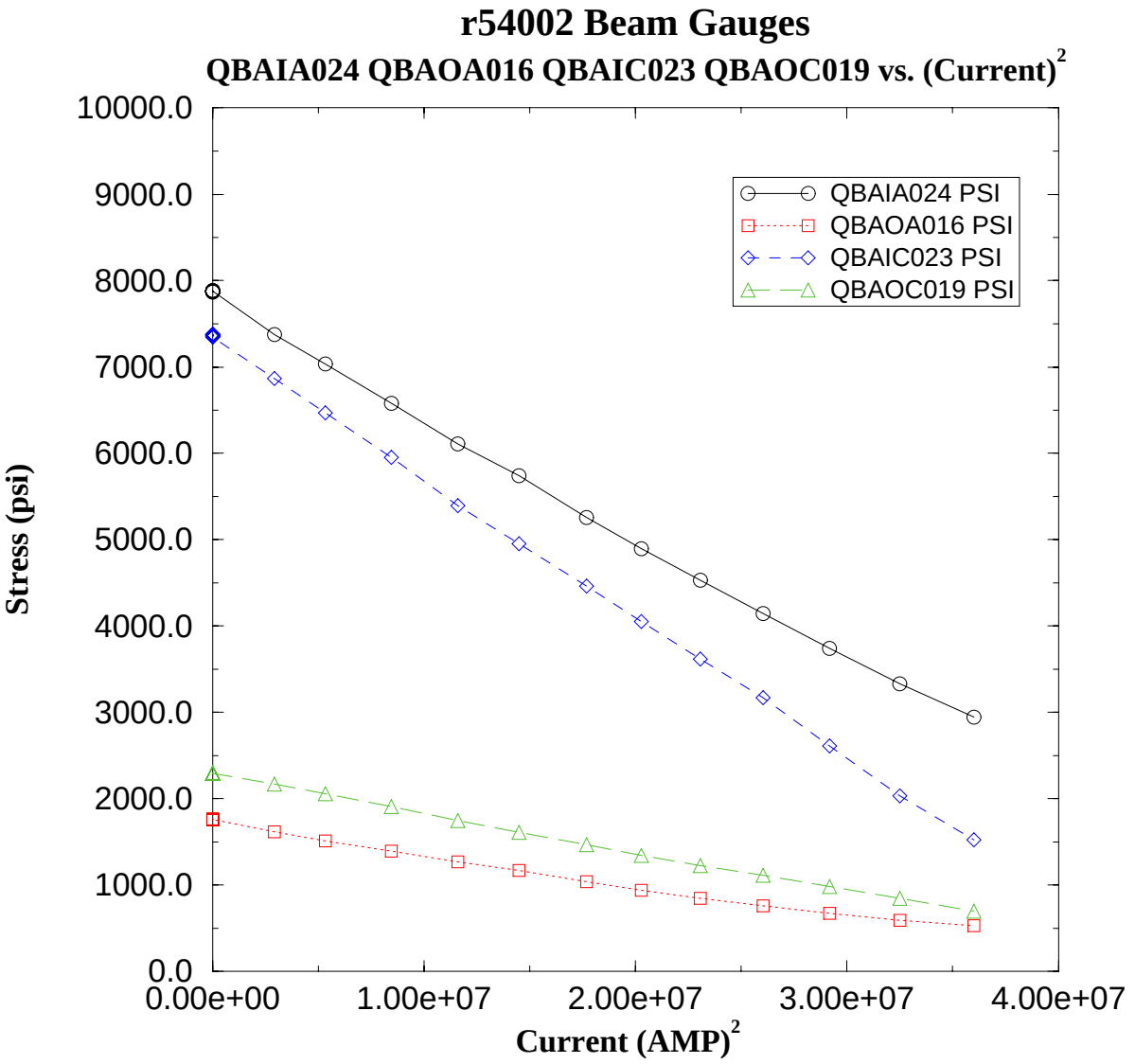

Figure 5.2: Coil stresses as recorded by inner and outer beam gauges as a function of square of the magnet current at 1.8K

Chapter 6

Splice resistance study

Measurement of the internal (inner-outer coil) splice resistances was carried out using precision HP 3458A DMM's to read splice voltage and magnet current (transductor voltage) and software developed to carry out the "Energy In - Energy Out" (EIEO) measurements (see chapter 8). The magnet was at 4.3K during these measurements. The voltage reading DMM was manually connected to the splice voltage taps using a 'breakout box' and the magnet current was then ramped to fixed values between 0 and 4000A. At each current step between 30 and 270 voltage and current readings were taken[1]. The splices were measured in the sequence A through D (corresponding to the quarter coil designations) with the measurements of splices C and D interrupted (hence they were repeated) by trips of the quench detection system (QDC#2). The EIEO program created a separate file for each current step. Table 6.1 provides a list of the files generated along with the initial and final comments added to the file by the operator.

As can be seen in Table 6.2, the first splice (A) measurements were performed at 1000A, 2000A, 3000A, and 4000A on the up ramp and at 1000A on the down ramp. Subsequent measurements used the current sequence: 0A, 1000A, 1500A, 2000A, 2500A, 3000A, 3500A, 4000A, 2000A, 1000A, 0A; this sequence provided a more complete set of data points to perform the

[1]The number of readings was set by the EIEO software used for this test; intially, 270 samples were taken a result of the parameters used in the program. Roughly midway through the measurements, we changed the program parameters to reduce the number of samples to 30 as part of an overall speed up of the measurement.

measurement. The data from each step were averaged to give the current and voltage and combined to form a voltage versus current plot. The resistance was then determined by a linear fit to these data (using the linear regression tool provided in xmgr, a Unix based data plotting routine.); the splice resistance is the slope of the line. The data analyzed in this manner are displayed in Figures 6.1 - 6.4. Table 6.1 summarizes the results of the measurements. The results include both the resistance derived from all the data and from the data after having been subjected to selection criteria to reject spurious readings. This is discussed in more detail below.

There are two aspects of the data of interest. First, the offset voltages (due to thermal emfs) are not small compared to the resistive voltages. The resistive component can only be determined by change in voltage with current (the slope method) due to these offsets. (Note: for three of the four splice taps, the voltage change is negative with respect to the change in current; this is due to the (random) manner in which the taps were connected to the DMM.)

The second feature of interest was the observation that, in a few cases, the error bars obtained from the average over data from a measurement were substantially larger than those from other measurements while the average values were in good agreement. Subsequent investigation of the data revealed bi-polar noise spikes in the voltage measurements and an occasional step in the current DMM voltage measurement. While the cause of these effects has not been understood at present, the bad readings appear to be spurious data not representative of the splice I-V behavior. Examples of these spurious readings are shown in Figures 6.5 and 6.6 which are the voltage and current DMM data from a measurement of splice C at 3000A. The data were reanalyzed, rejecting measurements with splice voltage or current reading 3 sigma or greater from the overall averages. The error bars were reduced substantially but neither the average values nor the resistances determined from the slopes changed appreciably.

The splice resistance varies from 1.9 $\mu\Omega$ to 4.2 $\mu\Omega$. As discussed above, the splices appear to play a role in limiting the quench performance of this magnet[2]. Subsequent investigation of the splice geometry indicates that the length of the solder joint between the two conductors is typically less than

[2]The mechanical stability of the splice and the coil ends are subjects for further examination. The cooling in the region of the splice also merits additional study.

4cm . The nominal pitch length of the low beta quadrupole cable is 7.6cm so that the nearly half of the strands would not be in direct contact in the splice. This fact alone would indicate that the overlap is roughly a factor of two too small.

Table 6.1: R54002 Splice Resistance Measurements

	Slope($n\Omega$)		Error($n\Omega$)		Corr. Coeff		Frac. Error	
Splice	raw	3σcut	raw	3σcut	raw	3σcut	raw	3σcut
A	3.91	3.92	2.50E-1	2.58E-1	0.9937	0.9935	6.39%	6.58%
B	1.88	1.87	7.00E-2	8.46E-2	0.9938	0.9919	3.72%	4.52%
C	2.82	2.82	9.10E-2	9.24E-2	0.9938	0.9937	3.23%	3.28%
D	4.15	4.15	5.64E-2	5.64E-2	0.9992	0.9990	1.23%	1.36%

Table 6.2: R54002 Splice Data Files

File Name	Initial Comment	Final Comment
/usr/vmtf/data/eleo/ts_5/		
r54002_300.dat_27Sep96_15:32:27	Outer to inner coil ramp slice (OIARS).	1000 Amps.
r54002_300.dat_27Sep96_15:37:47	2000 Amps	2000 amps
r54002_300.dat_27Sep96_15:41:33	3000 Amps.	3000 Amps.
r54002_300.dat_27Sep96_15:46:12	4000 Amps	4000 Amps.
r54002_300.dat_27Sep96_15:51:35	1000 Amps.	1000 Amps.
r54002_300.dat_27Sep96_16:36:45	Zero amp resistance data. OIBRS	zero amps.
r54002_300.dat_27Sep96_16:39:51	1000 Amps.	1000A splice outer-inner B
r54002_300.dat_27Sep96_16:42:22	1500A; outer-inner B	1500A inner-outer B
r54002_300.dat_27Sep96_16:44:26	2000A inner-outer B	2000A inner-outer B
r54002_300.dat_27Sep96_16:46:45	2500A inner-outer B	2500A inner-outer B
r54002_300.dat_27Sep96_16:49:19	3000A inner-outer B	3000A inner-outer B
r54002_300.dat_27Sep96_16:51:20	3500A inner-outer B	3500a inner-outer B
r54002_300.dat_27Sep96_16:53:23	4000A inner-outer B	4000A inner-outer B
r54002_300.dat_27Sep96_16:57:07	2000A (downramp) inner-outer B 2000A	(downramp) inner-outer B
r54002_300.dat_27Sep96_16:59:50	1000A (downramp) inner-outer B 1000A	(downramp) inner-outer B
r54002_300.dat_27Sep96_17:03:47	0 amps (downramp) inner-outer B	0 amp (downramp) inner-outer B
r54002_300.dat_27Sep96_17:06:03	0 amps inner-outer C	0 amps inner-outer C
r54002_300.dat_27Sep96_17:08:48	1000A inner-outer C	1000A inner-outer C
r54002_300.dat_27Sep96_17:10:59	1500A inner-outer C	1500A inner-outer C
r54002_300.dat_27Sep96_17:13:08	2000A inner-outer C	2000A inner-outer C
r54002_300.dat_27Sep96_17:15:19	2500A inner-outer C	2500A inner-outer C
r54002_300.dat_27Sep96_17:18:57	3000A inner-outer C	3000A inner-outer C
r54002_300.dat_27Sep96_17:20:54	3500A inner-outer C	Quench on QDC#2 magnet-Idot
r54002_450.dat_27Sep96_17:39:12	0 amp - repeat after QDC#2 trip inner-outer C	0 amps - repeat following QDC#2 trip - inner-outer C
r54002_100.dat_27Sep96_17:45:58	2000A (repeat following quench)	inner-outer C 2000A inner-outer C (repeat following QDC#2 trip)
r54002_100.dat_27Sep96_17:47:25	3000A inner-outer C (repeat)	3000A inner-outer C (repeat)
r54002_100.dat_27Sep96_17:48:46	3500A inner-outer C	3500A inner-outer C (repeat)
r54002_100.dat_27Sep96_17:50:08	4000A inner-outer C (repeat)	4000A inner-outer C (repeat
r54002_100.dat_27Sep96_17:52:20	2000A inner-outer C (repeat)	2000A inner-outer C (repeat) downramp
r54002_100.dat_27Sep96_17:53:57	1000A inner-outer C downramp (repeat)	1000A inner-outer C downramp (repeat)
r54002_100.dat_27Sep96_17:55:32	zero amps inner-outer C downramp(repeat)	zero amps inner-outer C downramp (repeat)
r54002_100.dat_27Sep96_18:08:26	zero amp inner-outer D	zero amp inner-outer D
r54002_100.dat_27Sep96_18:09:47	1000A inner-outer D	1000A inner-outer D
r54002_100.dat_27Sep96_18:10:47	1500A inner-outer D	1500A inner-outer D
r54002_100.dat_27Sep96_18:11:42	2000A inner-outer D	2000A inner-outer D
r54002_100.dat_27Sep96_18:12:39	2500A inner-outer D	2500A inner-outer D
r54002_100.dat_27Sep96_18:18:54	3000A inner-outer D	zero amp (repeat) inner-outer D following QDC #2 trip
r54002_100.dat_27Sep96_18:21:10	1000A inner-outer D(repeat - following	QDC#2 trip) 2000A inner-outer D (repeat)
r54002_100.dat_27Sep96_18:24:29	2000A inner-outer D (repeat)	2000A inner-outer D (repeat)
r54002_100.dat_27Sep96_18:26:26	3000A inner-outer D (repeat)	3000A inner-outer D (repeat)
r54002_100.dat_27Sep96_18:27:53	3500A inner-outer D (repeat)	3500A inner-outer D (repeat)
r54002_100.dat_27Sep96_18:29:25	4000A inner-outer D (repeat)	4000A inner-outer D (repeat)
r54002_100.dat_27Sep96_18:31:42	2000A inner-outer D downramp (repeat)	2000A inner-outer D downramp (repeat)
r54002_100.dat_27Sep96_18:33:25	1000A inner-outer D downramp (repeat)	1000A inner-outer D downramp(repeat)

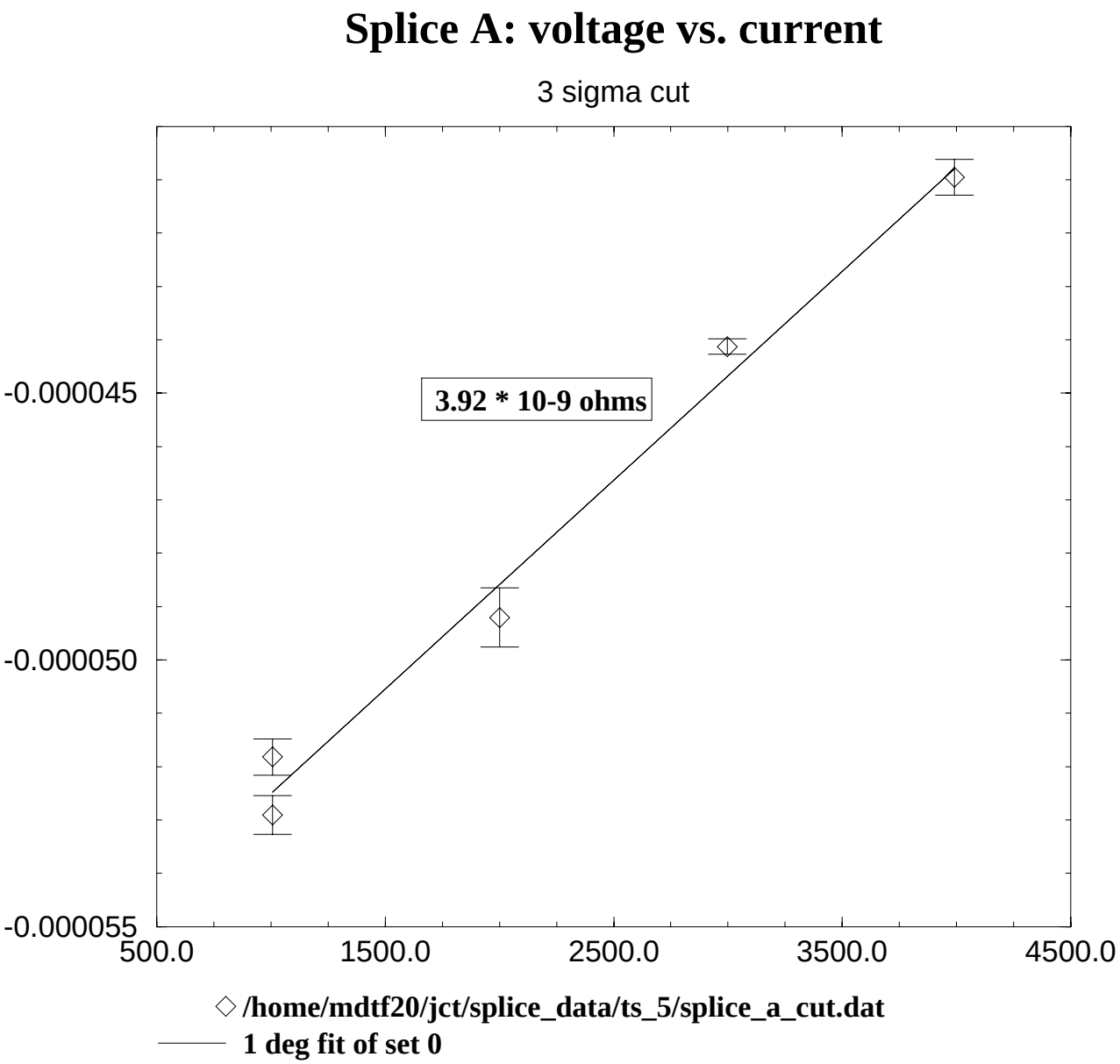

Figure 6.1: Voltage between splice (inner-to-outer Coil A) voltage taps as a function of magnet current

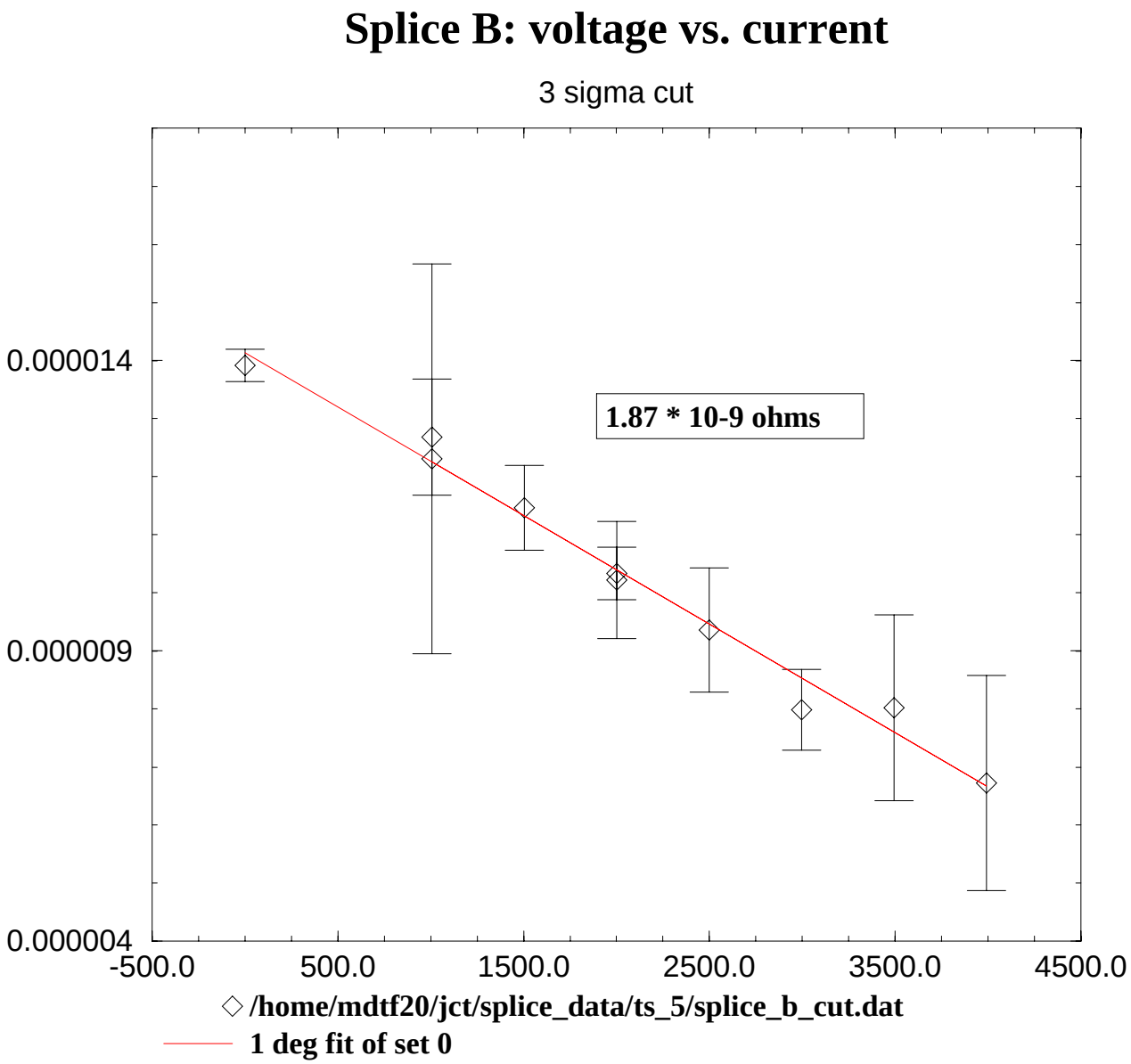

Figure 6.2: Voltage between splice (inner-to-outer Coil B) voltage taps as a function of magnet current

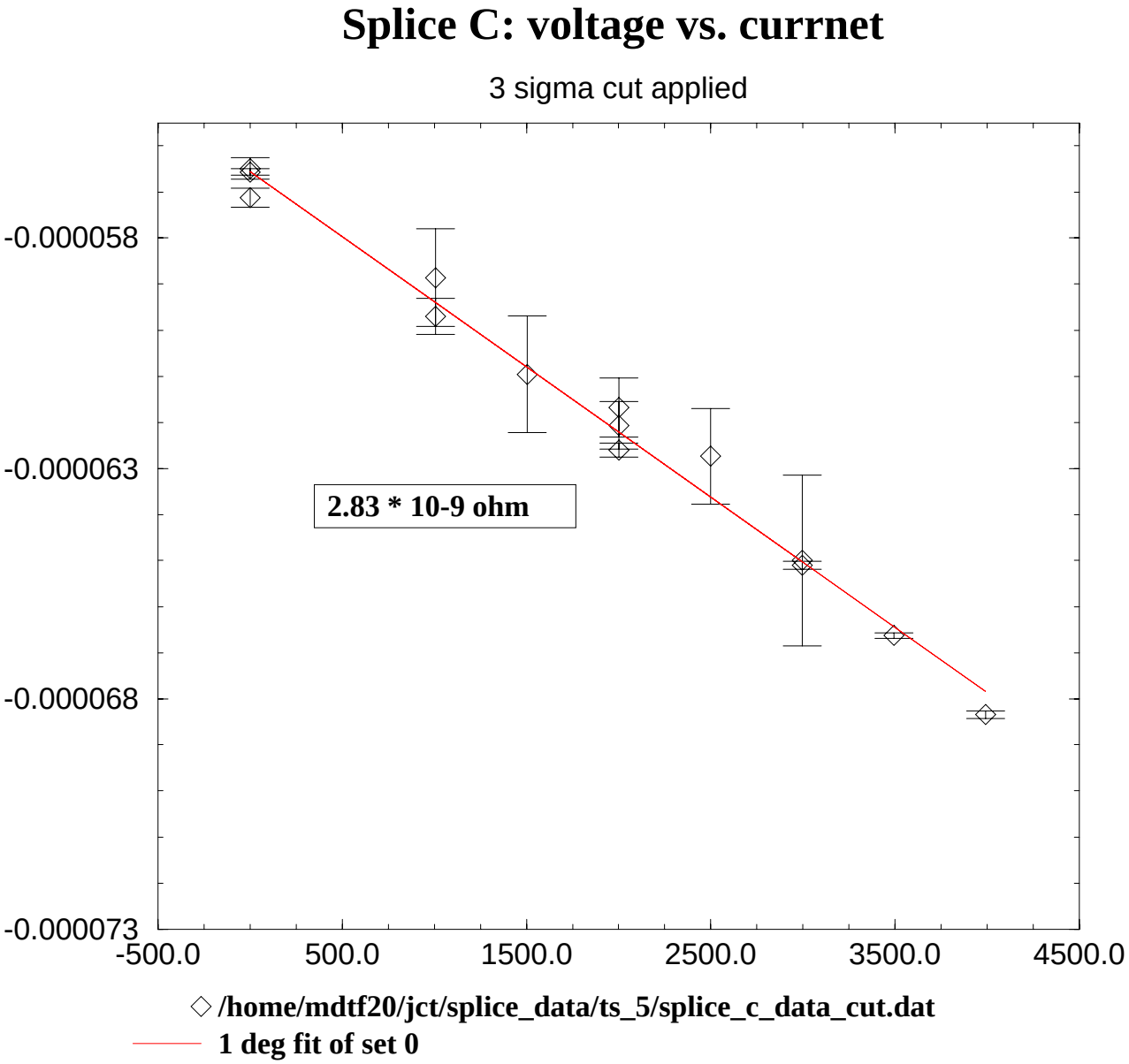

Figure 6.3: Voltage between splice (inner-to-outer Coil C) voltage taps as a function of magnet current

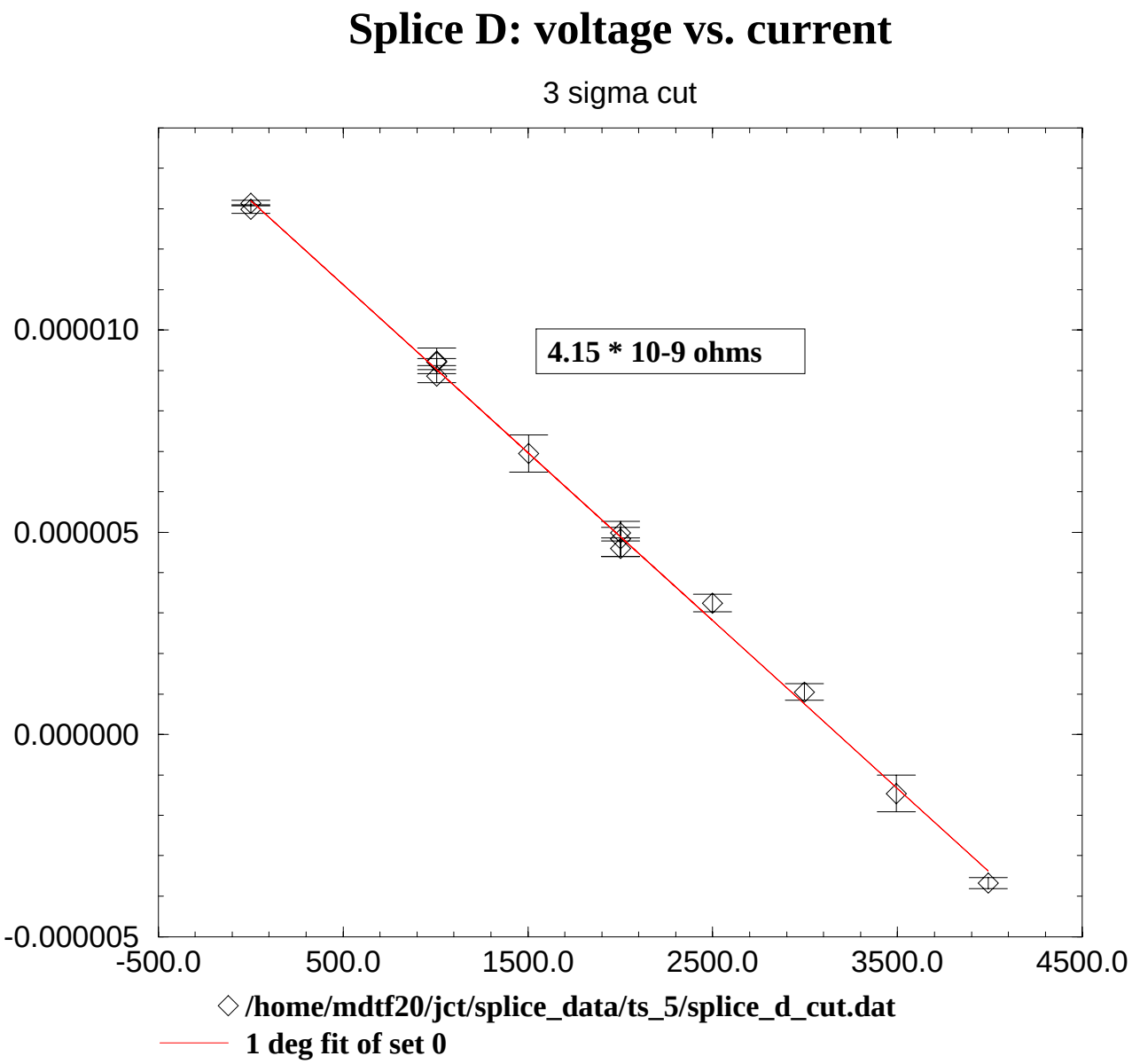

Figure 6.4: Voltage between splice (inner-to-outer Coil D) voltage taps as a function of magnet current

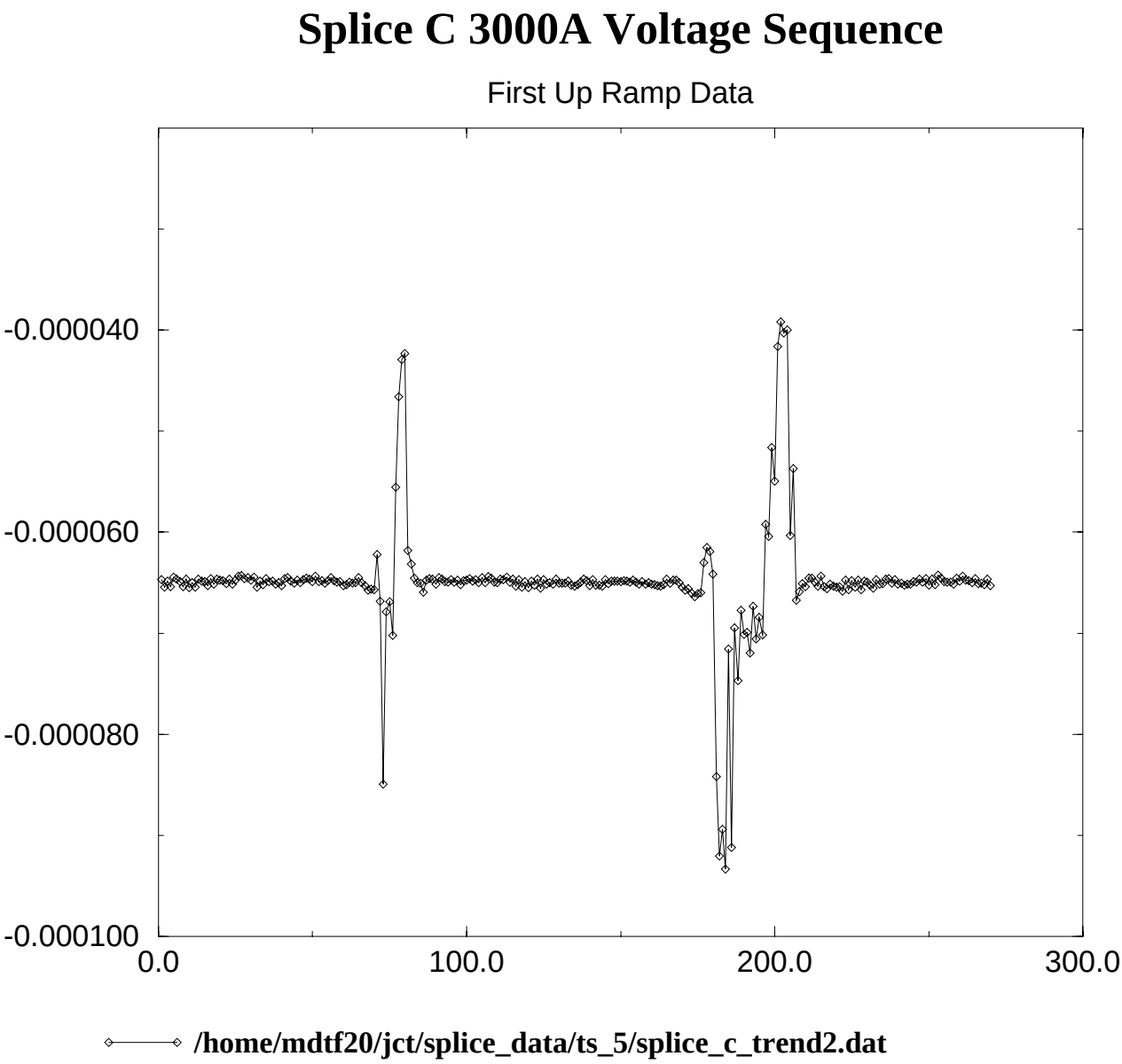

Figure 6.5: Bi-polar noise spikes in the voltage measurements

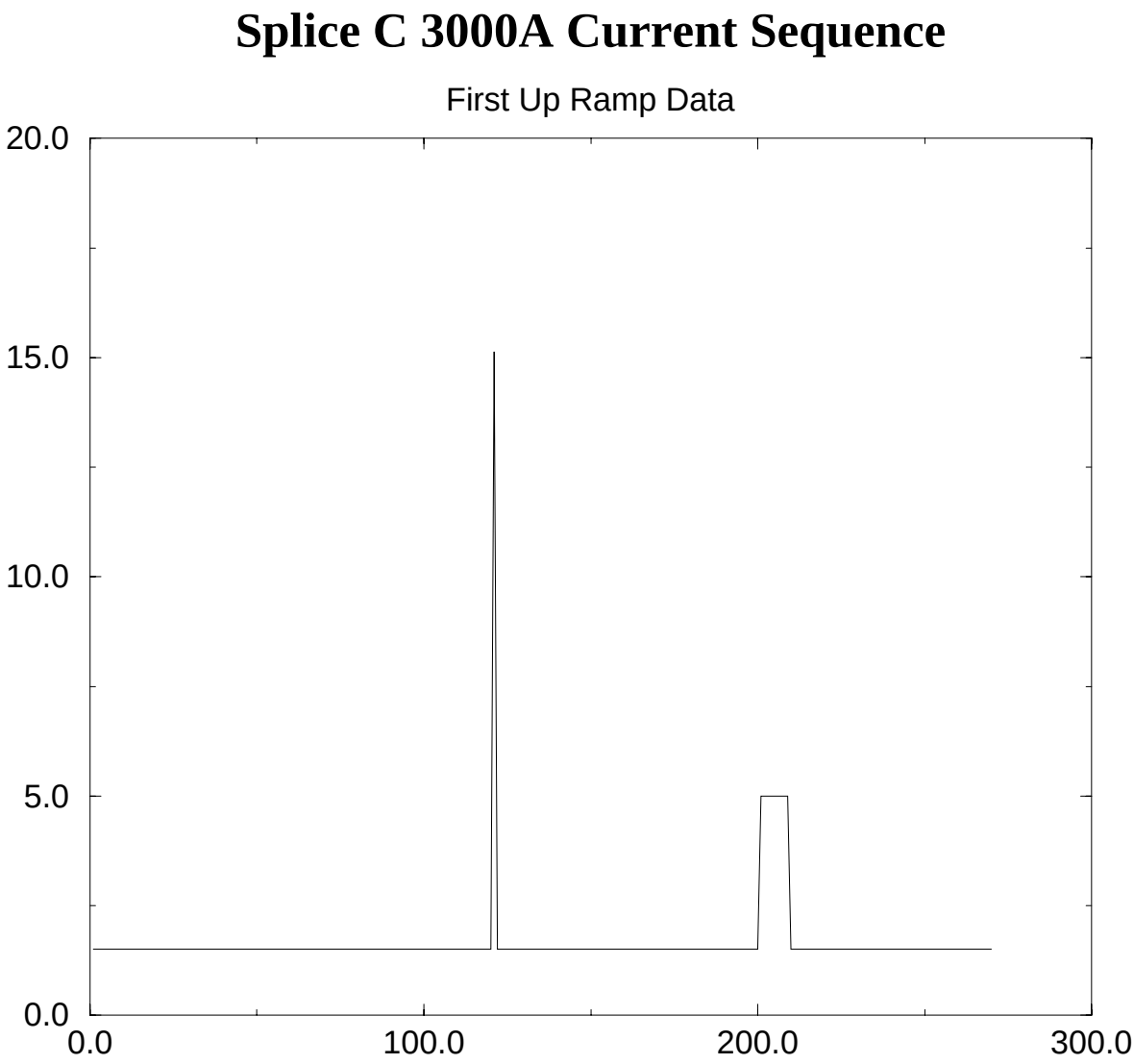

Figure 6.6: Noisy current reading

Chapter 7

RRR study

This chapter summarizes the residual resistance ratio (RRR) measurements. This measurement was performed at the beginning of the test period (see runplan in appendix A). In order to measure the RRR, we monitored the coil resistance and temperature dynamically during the cool down.

To measure the resistance we used the 4-wire measurement technique. A current of 1A was applied to the magnet using a Kepco Bipolar Operational Power Supply. To get the voltage readings, we used voltage taps that were attached to the coil (see chapter 1). The stability of the current source is shown in Fig 7.2 where we plotted the histogram of the measured value of the current source during the entire data taking. Both the voltage and current were measured using the HMTF cryogenic slow scan system [8] based on an HP3458A DMM.

To control the temperature we have instrumented several temperature sensors (Carbon-Glass and Platinum) in the vicinity of the magnet. The location of sensors are shown in Fig 7.1. The Carbon-Glass RTDs were calibrated over a temperature range of 1.5K to 300K. The measurement system interpolates between calibration points to generate the measured results. The Platinum RTDs are not calibrated as are the Carbon-Glass sensors. Their resistance is approximately linear and the deviation from linearity (European DIN standard in this case) can be determined well enough for RRR measurements. The accuracy of the Platinum sensor at 20K is .020K and .035K at 300K. To measure lower temperatures we used the Carbon-Glass RTDs. The accuracy of these sensors is .005K for temperatures less than 10K and .020K at 20K.

Fig 7.3- 7.4 shows the temperature and resistance measurements of the coils at room temperature. As mentioned earlier, the sensors are located in the vicinity of the coil but they are not attached to the coil. If the magnet is not in thermal equilibrium the sensors temperature reading will not reflect the temperature of the magnet. Before we took the room temperature measurements we let the magnet reach thermal equilibrium with the gas surrounding the coils. Therfore, the RMS values of the measurements should reflect the error of these measurements.

Although during the cool down we measured the temperature of the gas (liguid) and the resistance of the coil every minute, this was not sufficient to get reliable temperature resistance correspondence. The temperature of the magnet and the temperature of the sensors was different. To get the low temperature ($T \sim 10 - 20K$) value of the resistance of the quarter coils we took the lowest resistance values of the quarter coils that were logged during the cool down (see Fig 7.5). Below 9K the coil becomes superconducting, therfore data which were taken when part of the coil was already superconducting are not used in this analysis. There is a temperature gradient from the bottom of the coil to the top of the coil; however, below 20K the temperature dependence of the resistance of the copper is flat so it was sufficient to check that all four quarter coils' resistances are close to each other. The RRR measurements of the qurter coils are summarized in table 7.1.

Table 7.1: RRR results

Coil	RRR
whole	73
Coil A	69
Coil B	72
Coil C	71
Coil D	74

The resistance of a metal decreases approximately linearly with temperature as the metal is cooled below room temperature. At very low temperatures ($\sim$ 10K) the resistance reaches a constant value, which is determined by

the impurity level and other lattice defects (such as dislocations). Furthermore, in relatively pure metals, the temperature and impurity components of the total resistivity act independently of one another (Matthiessen's rule) and can be described with a universal function for each metal. If the low temperature and room temperature resistances are known then the resistance of the metal as a function of temperature can be easily calculated.

To make a self consistency check we compared the calculated [9] resistance temperature dependence values with a set of temperature and resistance data points taken when the magnet was gradually warming up (Fig 7.6). We plotted the whole coil resistance as a function of the temperature measured with the lead end and return end carbon glass temperature sensors. The parametrization curve using the measured RRR value do not agree with the measured data points. This is due to a temperature gradient between the lead end of the coil and the return end of the coil. Nevertheless that the shape of the resistance vs. temperature curve agrees with the parametrization.

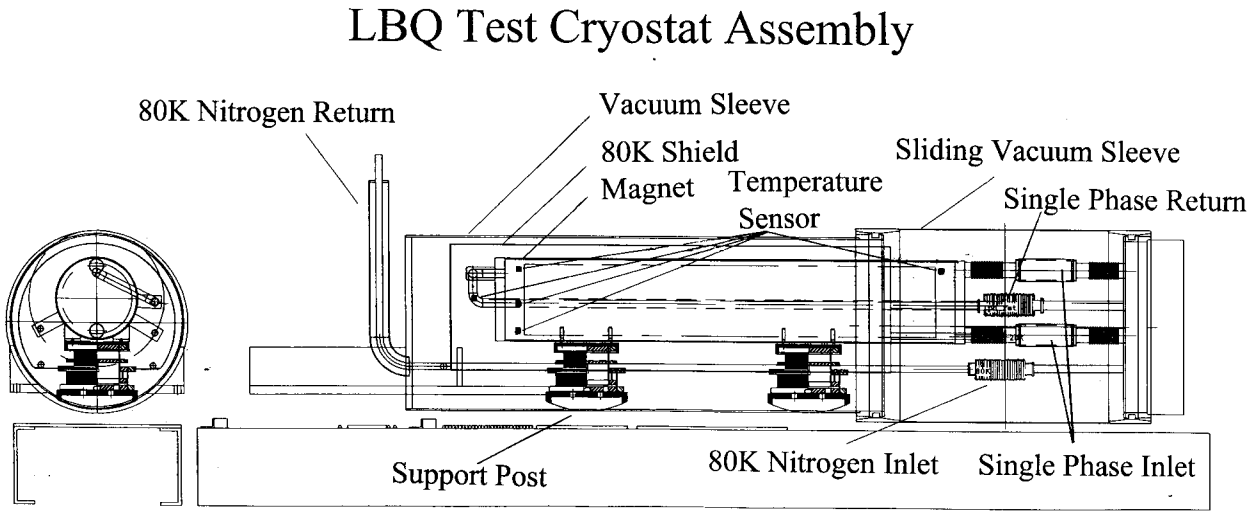

Figure 7.1: The location of the temperature sensors ralative to the cryostat and the magnet

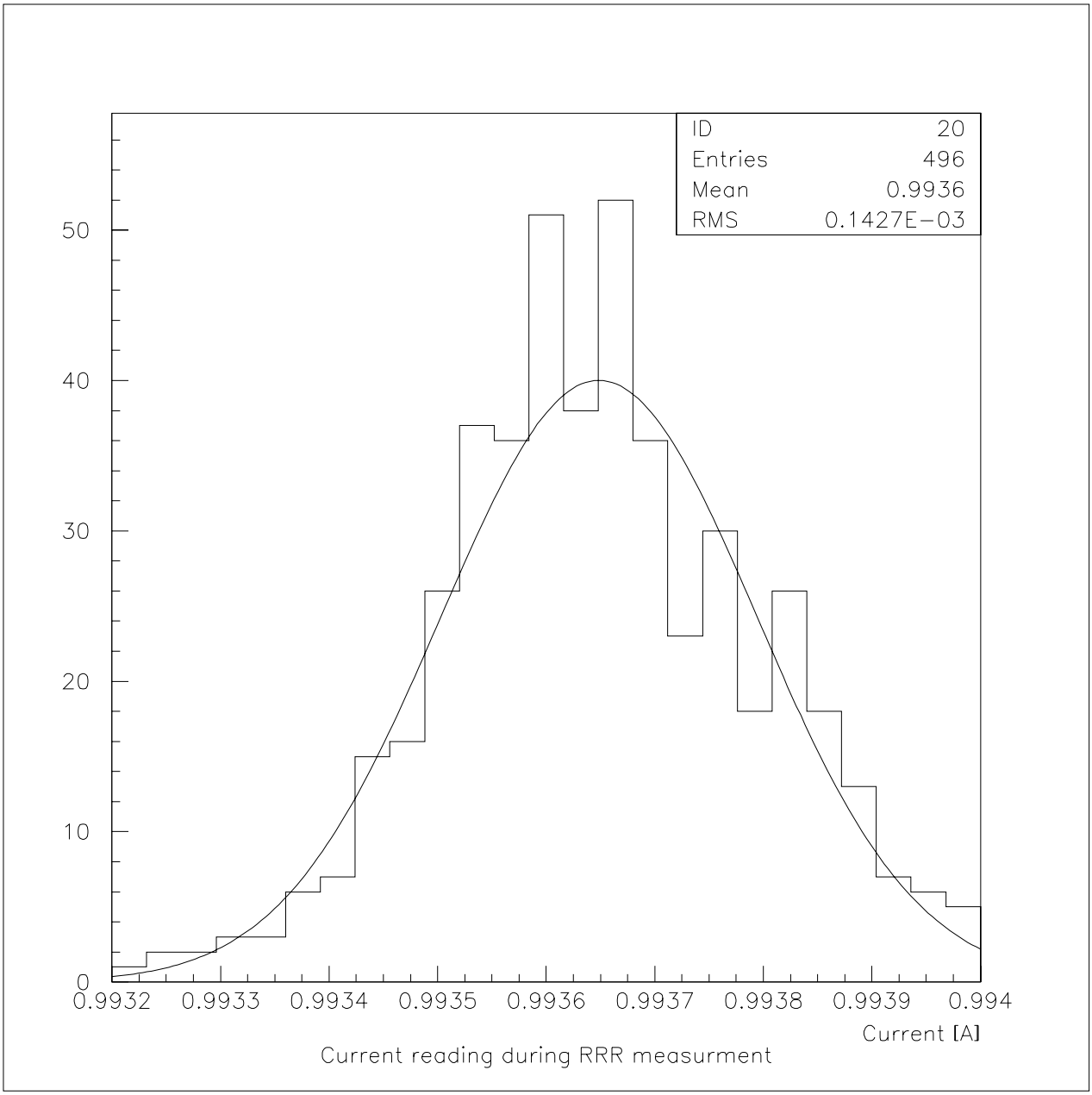

Figure 7.2: Variation of the output of the current source during the entire RRR data taking cycle

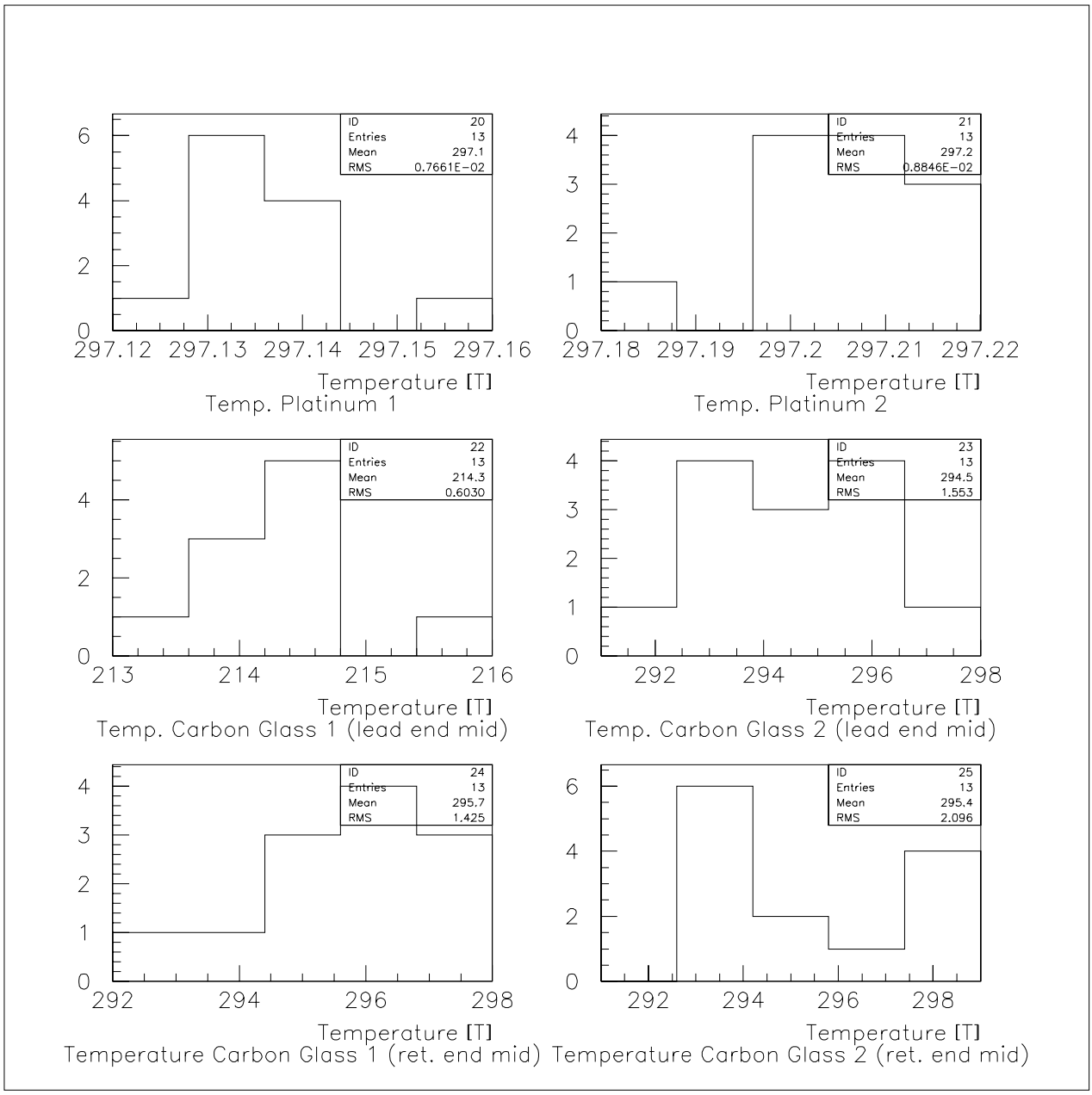

Figure 7.3: Temperature sensor readings at room temperature

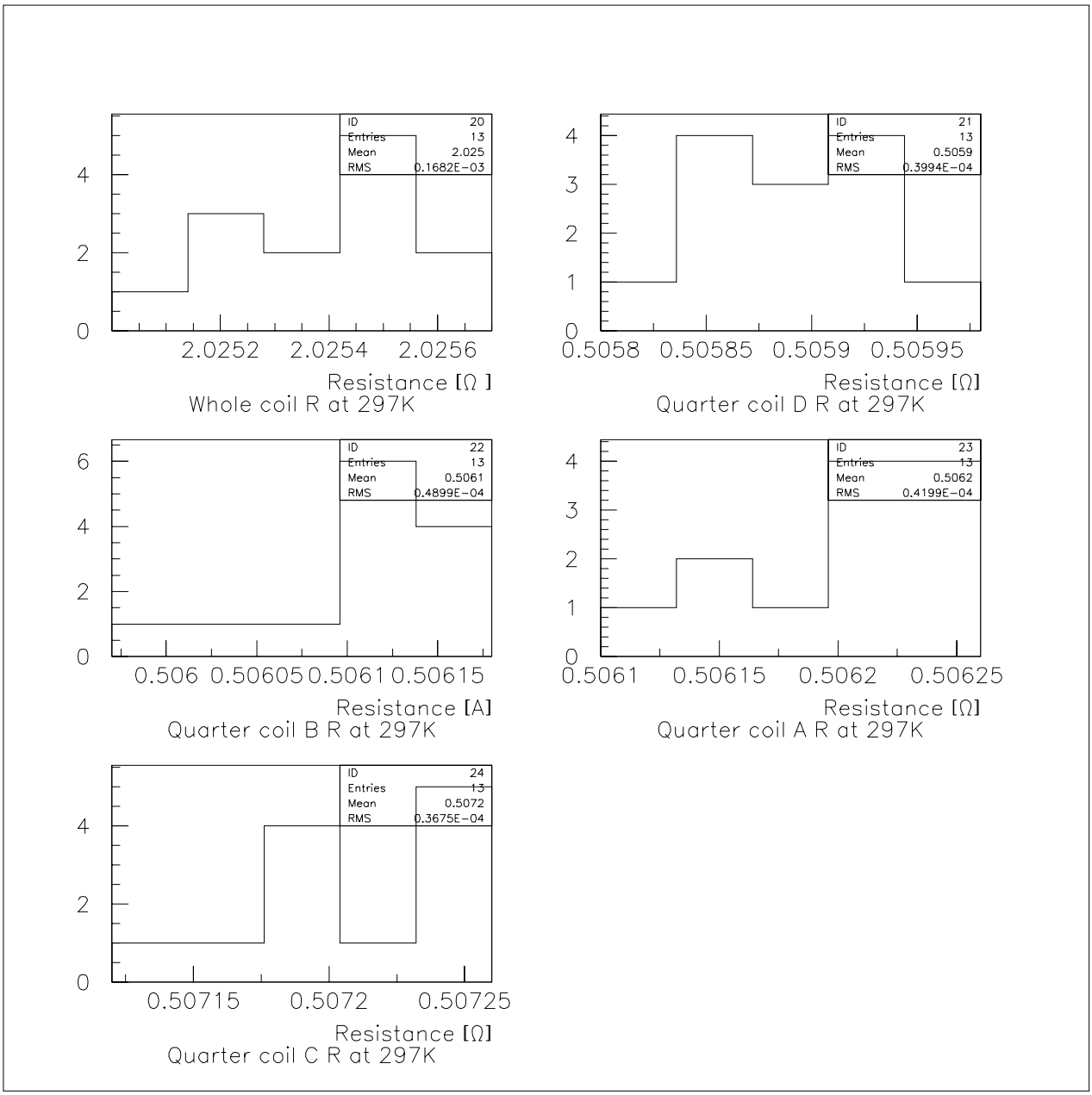

Figure 7.4: Room temperature resistance measurements of the coils

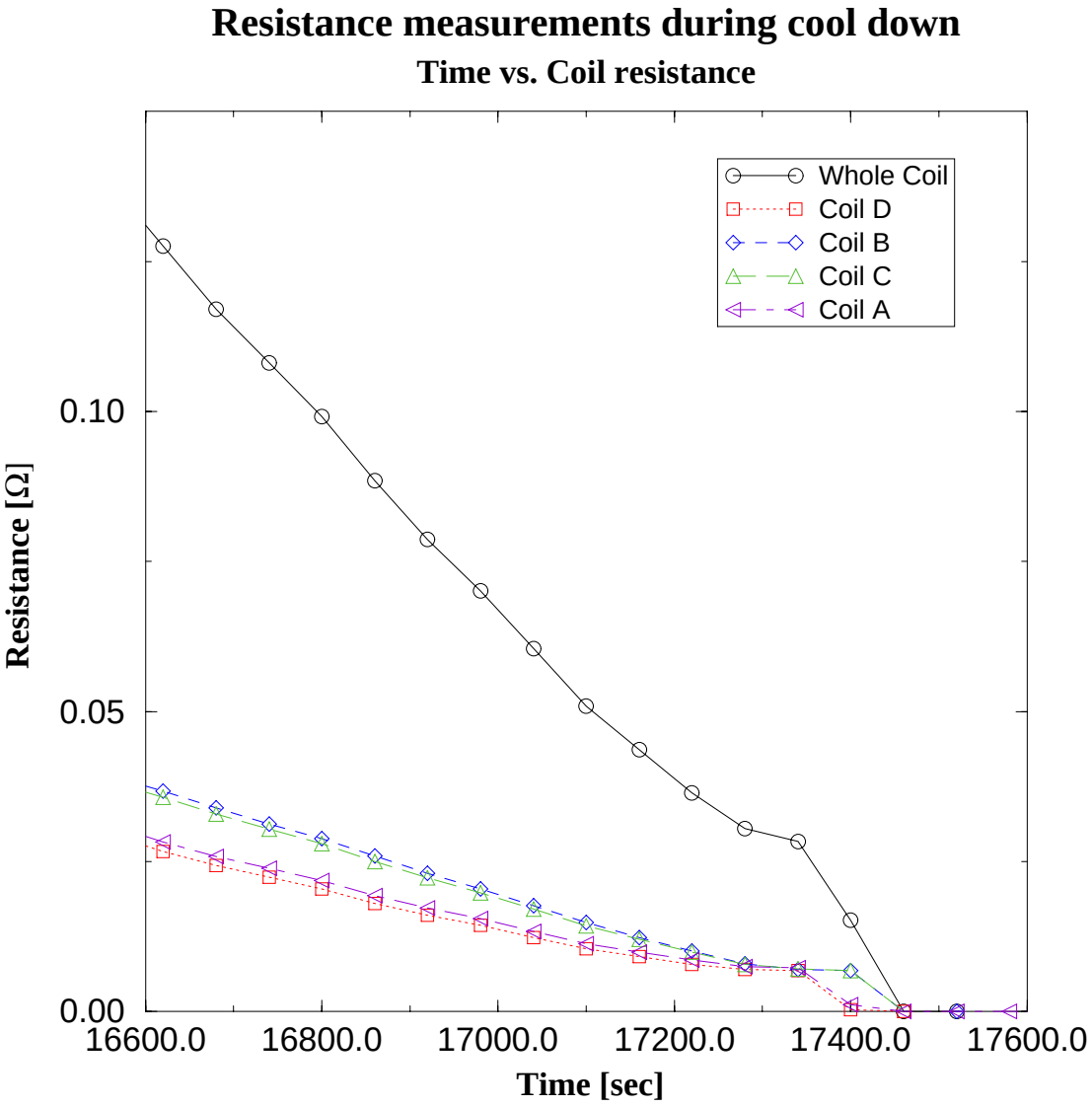

Figure 7.5: Resistance change during cool down

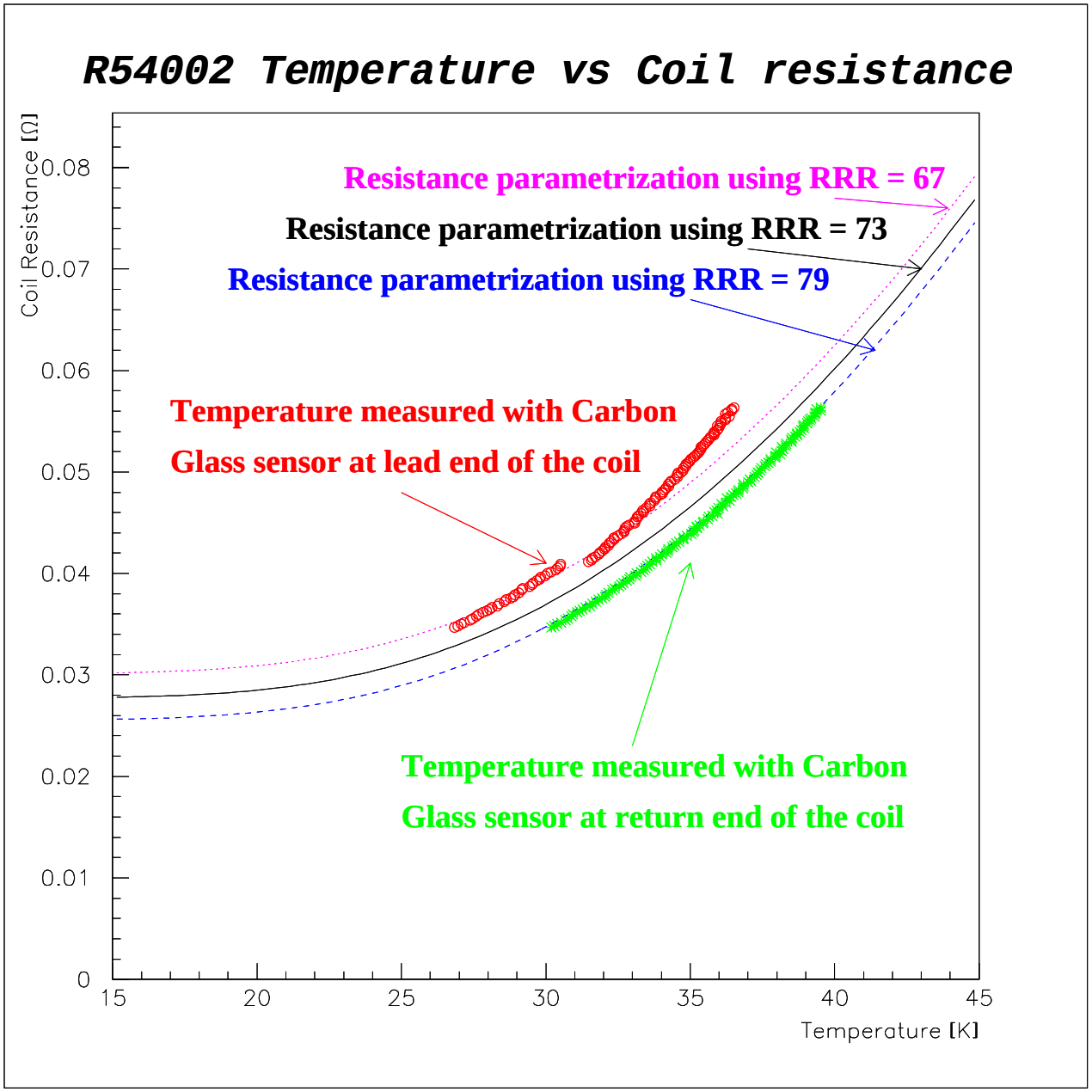

Figure 7.6: Resistance temperature dependence comparison with parametrization

Chapter 8

AC Loss Measurements

AC Loss measurements were performed on magnet R54002 at 3.8 and 1.8K. The data acquisition system, is similar in nature to that utilized in AC loss measurements on SSC magnets [10]. It consists of two fast, high sensitivity DMM's (HP Model 3458A) that are triggered nearly simultaneously (1.2 msec delay between master/slave). These DMM's record magnet current and voltage over an entire ramp cycle. The magnet current is measured using a Holec transducer, while the total magnet voltage is measured via the appropriate voltage taps. Low-pass input filters with a 1kHz cutoff frequency are used on both DMM's to reduce the effects of high frequency noise from the power supply.

The current profile used in the AC loss measurements is a modified sawtooth ramp, with a minimum current level of 500A and a maximum current level of 4000A. Ramp rates from 35 to 200 A/sec were used at 3.8 and 1.8K, while a ramp rate of 300 A/sec was additionally used only at 1.8K. The ramp profile includes flattops of 5 sec duration at I_{min} and I_{max}. The data were analyzed using the previous VAX analysis code, suitably modified for the particular magnet and run parameters, and ported to UNIX-based FORTRAN 77, and compiled and run on a Sparc IPX.

Results for the AC loss runs at 3.8K and 1.8K are shown in Fig 8.1-8.2 and Tables 8.1-8.2. In Figures 8.1-8.2, the loss per cycle (in Joules) is plotted against the ramp rate (in A/sec). Linear fits to the data provide a quantitative measure of the hysteresis and eddy current losses. The data from some runs show effects of amplifier saturation and anomalous noise "spikes", not unexpected in the shakedown of a new data acquisition system.

Loss calcualations based on these data are omitted form the figures shown here.

The resultant scatter in the data is considerably larger than that observed in previous measurements of SSC short model magnets. Amplifier saturation or obvious signal noise (other than a low-frequency oscillatory signal superimposed on the magnet voltage, that integrates to zero, and does not contribute to $\int V dt$, and thought to be due to effects of the Booster) does not appear to be present in these remaining data sets. Closer analysis shows that some magnet voltage data appear to exhibit a small, anomalous decrease in magnet voltage near the end of a ramp cycle, that does not seem to correspond to any discernible change in the magnet ramp rate. This is indicated in Fig 8.3, which shows the average magnet voltage decreasing in magnitude in the interval between 30.5 and 34.0 seconds, while Fig 8.4, which shows the magnet current during this same interval, does not show any obvious departure from a linear ramp. Small non-reproducible and non-symmetric fluctuations from the desired linear current ramp profile can lead to an additional loss/ramp cycle, and could be the source of much of the scatter in the data. Such "corrupted" ramp cycles can be identified by their larger value of $\int V dt$ over a complete cycle, which should, in the perfect case, be identically zero.

With this in mind, we can conclude that the calculated values for hysteresis and eddy current loss are not inconsistent with values calculated from similar measurements performed on SSC 50mm short model magnets.

Table 8.1: AC loss data at 3.8K

Ramp Rate [A/sec]	Loss [Joules]
34.83	219.68
49.73	164.87
149.24	423.62
149.24	230.41
199.05	239.92

Table 8.2: AC loss data at 1.8K

Ramp Rate [A/sec]	Loss [Joules]
34.83	249.02
49.73	228.12
49.73	246.6
49.73	292.04
49.72	312.86
149.24	292.86
149.24	369.37
199.05	333.42
199.05	415.61
199.05	414.52
298.67	587.50
298.67	397.44
298.67	394.28

Figure 8.1: Energy loss as a function of ramp rate for R54002 at 3.8K. The linear fit gives a hysteresis loss of about 184 J and an eddy current loss of about 0.62 J/A/sec

Figure 8.2: Energy loss as a function of ramp rate for R54002 at 1.8K. The linear fit gives a hysteresis loss of about 228 J and an eddy current loss of about 0.78 J/A/sec

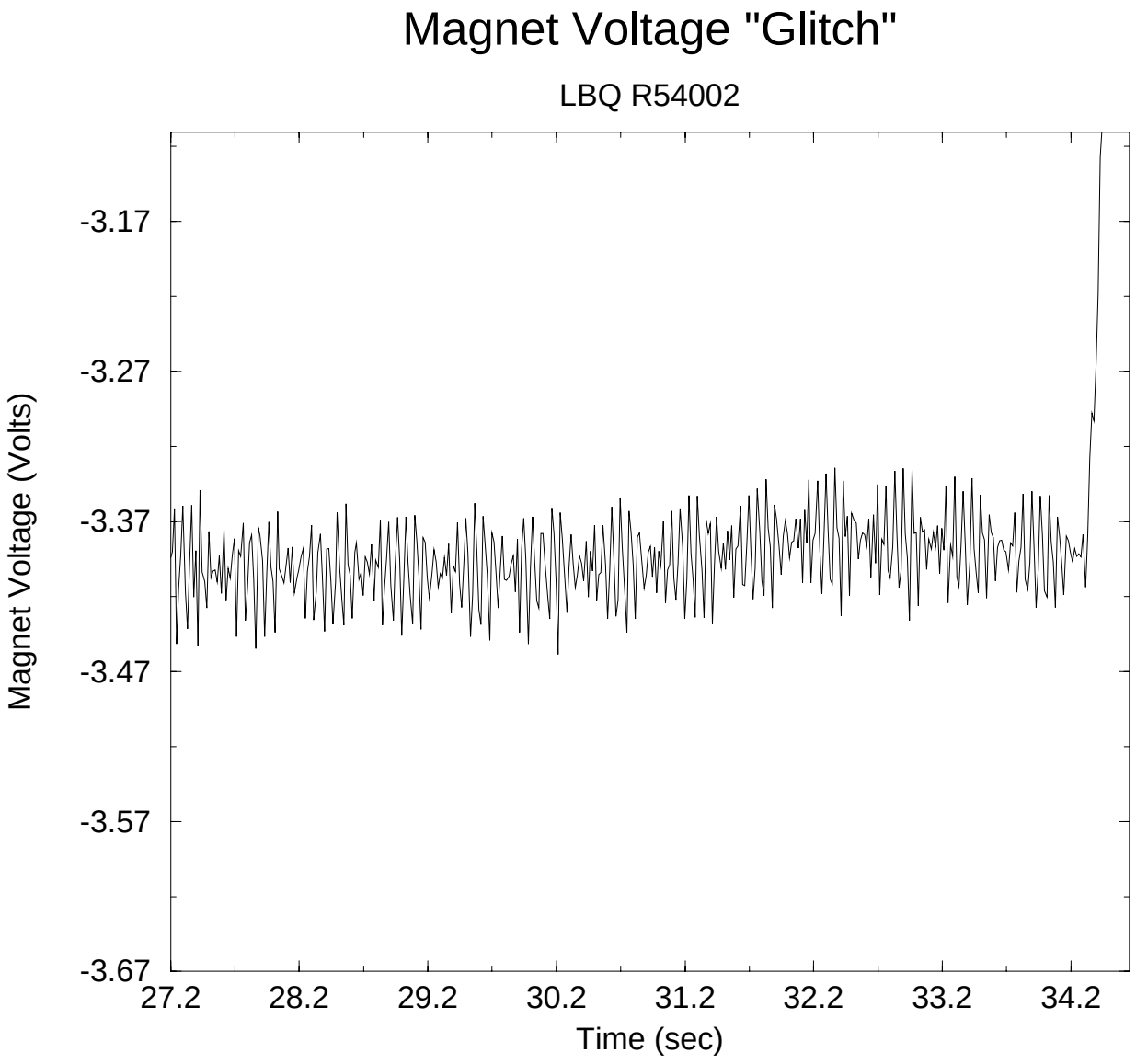

Figure 8.3: Average magnet voltage during current ramp

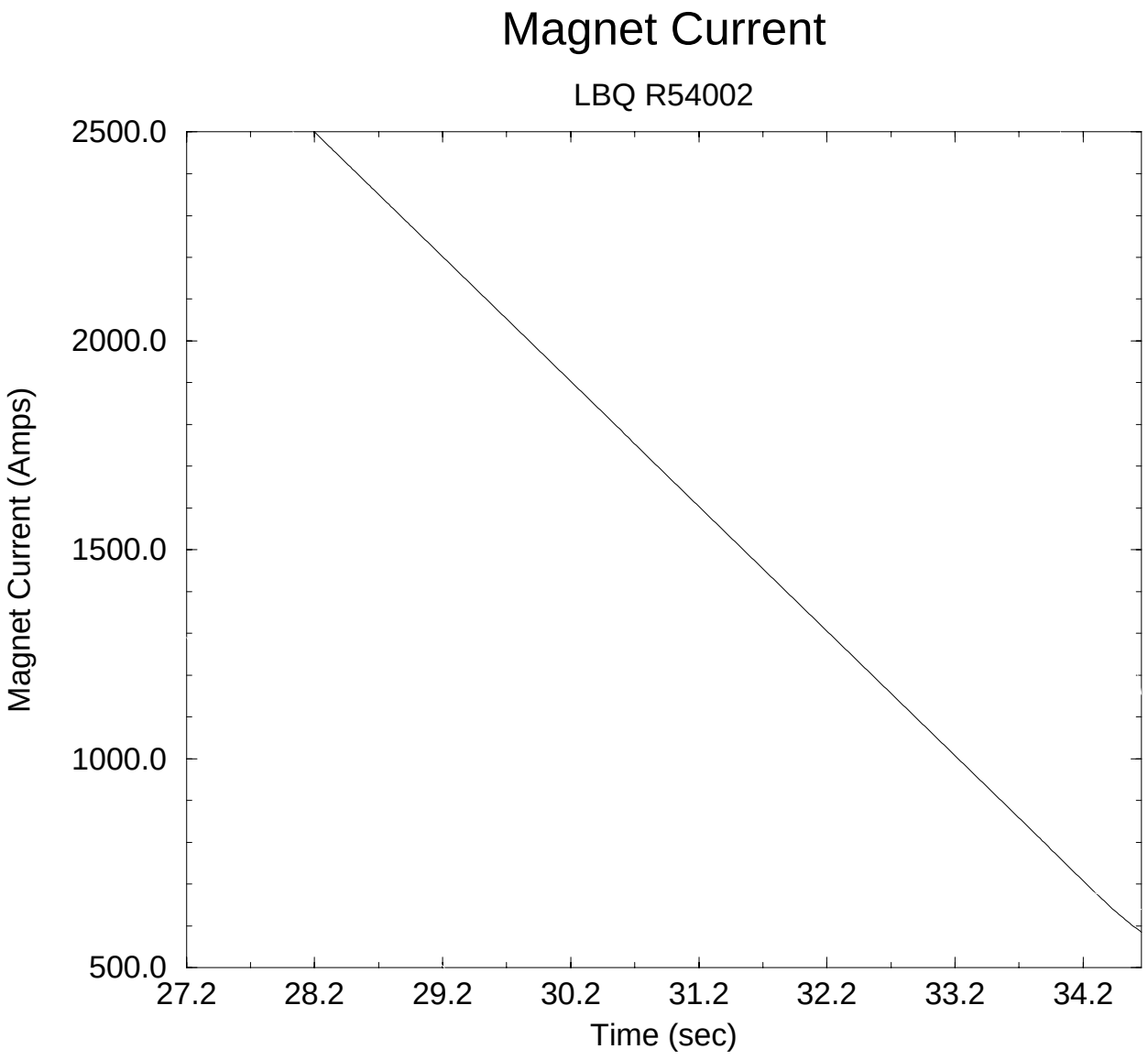

Figure 8.4: Magnet current as a function of time during a current ramp

Bibliography

[1] "D0 Low-β Quadrupole Requirements and Specifications #10," Fermilab Technical Support Section Internal Document, February 15, 1990

[2] T. Hegger, ANSYS Model of Low Beta Quad Mechanical Model # 4, TD 97-002

[3] Orris, D. HMTF instrumentation

[4] A. Ghosh, Private communication

[5] J. DiMarco, See /usr/vmtf/sh/qxplot.README file

[6] R. Bossert et. al., "Test of Fermilab Low-β quadrupoles", ASC'96, Pittsburg (1996)

[7] J.P.Ozelis, Results Of Strain Gauge Measurements For Low-Beta Quadrupole Mechanical model #4, with additional Observations", TS-96-017

[8] J. Nogiec, Private communication

[9] S.S. Kozub et.al."Thermal Conductivity and Electric Resistance of Composite Wires Based on HT-50", Cryogenics, Vol 32 ICEC Supplement (1992) p. 295

[10] J.P. Ozelis et. al., "AC Loss Measurements of Full size Model SSC Dipole Magnets at Fermilab" IEEE trans on Appl. Sup. Vol3 #1 (1993)

Appendix A

R54002 TEST PLAN

A.1 Outline

Thermal Cycle I

- Room Temperature Pretest and Cool down
  RRR
- At 4.3K 4 ATM Operation
  Pre-Current excitation Checkout
  1000 amp Dump test
  1500 amp Heater test
  Strain gauge runs
  Quench Plateau
  Ramp Rate Studies
- At 1.8K Operation
  Pre-current excitation Checkout
  1500 Heater test
  Strain gauge runs
  Quench Plateau
  Ramp rate studies

Heater studies

- 4.3K Heater studies
- Quench Current vs. temperature
- Additional studies as needed

  Splice resistant measurement Energy loss measurement

Thermal Cycle II

- At 1.8K Operation, few quenches

A.2 Thermal cycle I

A.2.1 Room Temperature Pretest/Cooldown

1. Follow Present procedures for Strain gauge, voltage taps, thermometer, and heater validation. Procedures include:
   (a) 4 wire measurement of all strain gages
   (b) 5 amps across magnet, measure voltage across taps Measure magnet resistance for RRR
   (c) 4 wire heater resistance, system resistance
2. Record at least 10 strain gage readings at room temperature, check values with post assembly readings
3. Set strain gage and thermometer readings to 10 minute intervals
4. Cool to 4.35 K , 4 ATMs with unrestricted cooldown and RRR studies at $\sim$10 K. Place 5 amps through magnet, measure voltage across magnet

A.2.2 At 4.3K 4 ATM Operation

1. Cold electrical tests prior to magnet testing (**ET 12 hours**)
   (a) Check magnet resistance to ground
   (b) Hi pot (5 or 4 ATM helium)
   (c) 0 A strain gauge readings
   (d) Protect magnet with a 100 mΩ dump resistor (109 mΩ effective system resistance).
   (e) Heater Pretests
      i. Set dump delay to 1 sec, no heater firing delay
      ii. Set data loggers with V, I heaters to 50% pre quench window 400 Hz clock
      iii. Check heater and heater system resistance using 4 wire techniques. System resistance should be approximately 2.5 Ω. System capacitance should be set to approximately 12 mF.
      iv. Verify that heaters are wired in parallel check system continuity
      v. Fire Heaters from quench detection circuits with SSC program operating. Verify RC, V heaters, I heaters form data logger plots
   (f) Balance quench detection circuitry
      i. Set dump delay to 0 sec
      ii. Set data logger sampling frequencies and pre-quench windows: all the data loggers at 400 Hz and 25% pre-quench
      iii. sawtooth ramps between 100 A and 200 A at 50 A/sec.
      iv. Verify thresholds with setting in SSC parameter file
   (g) Manual trip at 1000 A.
      i. Set dump resistance to 100 mΩ.
      ii. Delay heater firing to 1 sec dump delay = 0 sec. Check L/R, look at all data logger voltage signals; compare Vmax to I*Rdump
2. Quench Heater Protection studies (**ET 4 hours**)

(a) Set dump resistor delay to 50 ms, no heater delay, no power supply phase off delay

(b) Set data logger to 400 Hz and 50% prequench window

(c) At 1500A magnet current, determine voltage required to quench both heaters with t_{fn} ¡ 200 ms

(d) If MIITS o.k dump resistor to 100 ms, delay heater firing to 50 ms

3. Strain gauge run (**ET 4 hours**)

(a) Dump resistor set to 100 mΩ, 100 ms delay , delay heater to 50 ms, heater value as perr A.2.2 2.d

(b) Set data logger sampling frequencies and pre-quench windows:

i. a) data loggers non-multiple vtap: 1 kHz and 25% pre-quench.

ii. b) data loggers multiple v tap: 2 kHz and 50% pre-quench.

(c) At Ramp rate = 16 A /sec. :

Take strain gauge runs, one file per current loop, using the sequences of currents below. Take data at all currents on the way up, and for the currents marked "*" on the way down. S.G. readings taken in 10 intervals of I^2 from 0 to 5400A.

i. Run 1: 0*, 1700, 2300*,2900,3400*, 3800 A

ii. Run 2: 0*, 1700, 2300*,2900,3400*, 3800, 4200A

iii. Run 3: 0*, 1700, 2300*,2900,3400*, 3800, 4200*, 4500A

iv. Run 4: 0*, 1700, 2300*,2900,3400*, 3800, 4200*, 4500, 4800*A

v. Run 5: 0*, 1700, 2300*,2900,3400*, 3800, 4200*, 4500, 4800*, 5100A

vi. Run 6: 0*, 1700, 2300*,2900,3400*, 3800, 4200*, 4500, 4800*, 5100, 5400A

Note: After Run 1, expect quench during strain gage run

4. Quench plateau. (**ET 12 hours**)

With ramp rate = 16 A/sec, train the magnet until 4 plateau quenches have occurred. Do not do more than 10 quenches. The predicted short sample limit currents (inner coil) is 5400 A.

5. Take a strain gauge run to Iplateau - 100 A. (**ET 30 min**)

6. RAMP RATE dependence studies. (**ET 6 hours**)

   Ramp to quench at 300 a/s, 200, a/s, 150 a/s, 100 a/s (depend on the quench plateau)

A.2.3 At 1.8K Operation

1. Cold Electrical tests prior to current excitation (**ET 8 hours**) Repeat section A.2.2 1.c,d,e

2. Quench Heater Protection studies (**ET 4 hours**) Repeat Section A.2.2 1.a,b,c,d

3. Strain gauge run (**ET 4 hours**)

   (a) Repeat Section A.2.2 3.a

   (b) Set data logger sampling frequencies and pre-quench windows:

      i. data loggers non-multiple vtap: 1 kHz and 25% pre-quench.

      ii. data loggers multiple v tap: 2 kHz and 50% pre-quench.

   (c) At Ramp rate = 16 A /sec. : Take strain gauge runs, one file per current loop, using the sequences of currents below. Take data at all currents on the way up, and for the currents marked "*" on the way down.

      i. Run 1: 0*, 1700, 2400*,2900,3400*, 3800, 4200*, 4500A

      ii. Run 2: 0*, 1700, 2400*,2900,3400*, 3800, 4200*, 4500, 4800*, 5100A

      iii. Run 3: 0*, 1700, 2400*,2900,3400*, 3800, 4200*, 4500, 4800*, 5100, 5400A

      iv. Run 4: 0*, 1700, 2400*,2900,3400*, 3800, 4200*, 4500, 4800*, 5100, 5400, 5700A

      v. Run 5: 0*, 1700, 2400*,2900,3400*, 3800, 4200*, 4500, 4800*, 5100, 5400*, 700, 6000A

      vi. Run 6: 0*, 1700, 2400*,2900,3400*, 3800, 4200*, 4500, 4800*, 5100, 5400*, 5700A, 6000A, 6200A

vii. Run 7: 0*, 1700, 2400*,2900,3400*, 3800, 4200*, 4500, 4800*, 5100, 5400*, 5700A, 6000A, 6200A, 6400A

viii. Run 8: 0*, 1700, 2400*,2900,3400*, 3800, 4200*, 4500, 4800*, 5100, 5400*, 5700A, 6000A, 6200A, 6400A, 6600A

ix. Run 9: 0*, 1700, 2400*,2900,3400*, 3800, 4200*, 4500, 4800*, 5100, 5400*, 5700A, 6000A, 6200A, 6400A, 6600, 6800A etc...

4. Quench plateau. (**ET 16 hours**)

   With ramp rate = 16 A/sec, train the magnet until 4 plateau quenches have occurred. Do not do more than 10 quenches (only if magnet shows interesting behavior). The predicted short sample limit currents (inner coil) is 7150 A.

5. Take a strain gauge run to Iplateau - 100 A. (**ET 30 min**) Scan strain gauges during ramping the magnet up

6. RAMP RATE dependence studies. (**ET 10 hours**)

   Ramp to quench at 25 a/s, 50 a/s, 75 a/s, 100 a/s, 150, a/s, 200 a/s, 300 a/s

7. Heater studies at 1.8K (**ET 16 hours**)

   Decide what I_c value to use !

   (a) Set dump resistor delay to 50 ms, no heater delay, no power supply phase off delay

   (b) Set data logger to 400 Hz and 50% prequench window

   (c) At 1500A magnet current determine Vmin for quench (if it was not done at 2)) . Fire heaters at additional voltage values:

   200, 250, 300 (choose the values to start from Vmin and to be linear with the deposited energy). DO NOT EXCEDE MAXIMUM HFU VOLTAGE

   (d) Between 2800-3200 amps ($I/I_c = 0.4$) determine Vmin for quench.

   (e) Between 5000-5400 amps ($I/I_c = 0.7$) determine Vmin for quench.

   (f) Between 6300-6600 amps ($I/I_c = 0.9$) determine Vmin for quench Fire heaters at additional voltage values:

100, 150, 175, 200, 250 (choose the values to start from Vmin and to be linear with the deposited energy). DO NOT EXCEDE MAXIMUM HFU VOLTAGE

A.2.4 4.3 K Heater Study

Decide what I/I_c value to use ! (**ET 16 hours**)

1. Set dump resistor delay to 50 ms, no heater delay, no power supply phase off delay

2. Set data logger to 400 Hz and 50% pre-quench window

3. At 1000A magnet current determine Vmin for quench (if it was not done at II. e)) . Fire heaters at additional voltage values:

   200, 250, 300 (choose the values to start from Vmin and be linear with the deposited energy). DO NOT EXCEDE MAXIMUM HFU VOLTAGE

4. Between 2000-2500 amps ($I/I_c = 0.4$) determine Vmin for quench.

5. Between 3600-4000 amps ($I/I_c = 0.7$) determine Vmin for quench.

6. Between 4700-5000 amps ($I/I_c = 0.9$) determine Vmin for quench Fire heaters at additional voltage values:

   100, 150, 175, 200, 250 (choose the values to start from Vmin and be linear with the deposited energy). DO NOT EXCEDE MAXIMUM HFU VOLTAGE

A.2.5 Quench Current vs. temperature

Ramp magnet to quench at 16 a/s at the following temperatures (**ET 8 hours**)

4.2K, 3.7K, 3.2K, 2.7K, 2.2K
should not be exact value (.2 K)

A.2.6 Additional Tests

- Splice resistance measurements (**ET 2 hours**) Measure resistance with DVM at 1000A, 2000A, 3000A
- Energy loss measurement (at 1.8K) (**ET 8 hours**)

  Ramp the magnet up to 5000A from 500A wait 5 sec then ramp down. Repeat this at least three times. Monitor coil voltages.

  Change the ramp rate between 30 - 300 A/s (30A/s, 50 A/s, 100 A/s, 150 A/s, 200 A/s, 250 A/s, 300 A/s)

A.3 Thermal cycle II

Quench the magnet few times

Appendix B

Data file summary

The binary quench data were stored on the VAX and later converted to ASCII files for storage on a UNIX workstation. The location of the files on the VAX are: MDTF00::SSC$ROOT:[DATA.QUENCH]R54002.*. In the table we listed only the * values. the MTF UNIX cluster: /vmtf/analysis/quench_data/lbqrd2/r54002_*.

File	Date	Time	Nom. Temp	Ramp Rate	Current	Q D C	MIITs	Comments
QB000	19-Sep-96	14:51:18	4.3		-11.3	1		ZERO AMPERE TRIP TO CHECK THE HEATERS
QB001	19-Sep-96	15:37:41	4.3		986.5	1	0.08	1000A MANUAL TRTIP TO CHECK INSTRUMENTATION
QB002	20-Sep-96	15:06:02	4.3		986.5	1		"2ND 1000A TRIPP, TTO CHECK INSTRUMENTATION"
QB003	20-Sep-96	16:51:51	4.3		1485.4	1	0.32	"1500A HEATER FIRING QUENCH, HEATER VOLTAGE 225V"
QB004	20-Sep-96	18:22:20	4.3		2859.9	2	1.05	FIRST STRAIN GAUGE RUN
QB005	20-Sep-96	20:34:39	4.3	16	4694.2	1	3.27	FIRST QUENCH AT 4.3K
QB006	20-Sep-96	23:51:03	4.3	16	4767.5	1	3.32	SECOND QUENCH AT 4.3K
QB007	21-Sep-96	9:18:17	4.3	16	4811.5	1	3.44	RAMP TO QUENCH @16 A/SEC. TEMPERATURE IS 4.2K. 3RD QUENCH.
QB008	21-Sep-96	10:25:55	4.3	16	4748.0	1	3.28	"4TH QUENCH, 16A/S, 4.3K"
QB009	21-Sep-96	11:55:36	4.3	32	4782.2	1	3.37	RAMP TO QUENCH AT 32A/SEC; QUENCH #5 `AT 4.3K
QB010	21-Sep-96	13:40:23	4.3	300	2634.9	1	1.83 2.62	300A/SEC RAMP RATE - QUENCH #6 AT 4.3K
QB011	21-Sep-96	14:07:35	4.3	200	3525.1	1	2.62	RAMP RATE QUENCH AT 200 A/SEC - 7TH QUENCH AT 4.3K
QB012	21-Sep-96	14:35:14	4.3	150	4019.1	1	2.92	RAMP RATE = 150A/SEC QUENCH #8 AT 4.3K
QB013	21-Sep-96	15:21:01	4.3	100	4513.2	1	3.25	RAMP R`ATE = 100A/SEC; QUENCH #9 AT 4.3K
QB014	21-Sep-96	17:52:17	4.3	64	4684.4	1	3.27	"64A/SEC , 4.3K, 10TH QUENCH"
QB015	22-Sep-96	10:09:10	1.8	0	1485.4	1	0.32	"HEATER TEST AT 1.73K, HFU WAS SET TO 275V, 1500A"

File	Date	Time	Nom. Temp	Ramp Rate	Current	Q D C	MIITs	Comments
QB017	22-Sep-96	13:07:40	1.8	16	5711.6	1	4.79	"11TH QUENCH, SUPERFLUID TEMP, 16A/SEC"
QB018	22-Sep-96	15:40:09	1.8	16	5956.1	1	4.21	2ND SPONTANEOUS QUENCH AT 1.8K; 12TH OVERALL
QB019	22-Sep-96	17:20:02	1.8	16	5638.2	1	4.66	"1.8K, 16A/SEC 13TH QUENCH OVERALL"
QB020	22-Sep-96	18:40:49	1.8	16	6024.6	1	4.21	4TH S.F. QUENCH. 14TH QUENCH OVERALL; 16A/S AT 1.8K
QB021	22-Sep-96	20:10:34	1.8	16	5965.9	1	4.21	5TH QUENCH IN SUPER FLUID. 15TH QUENCH OVERALL; 16A/sec
QB022	22-Sep-96	21:27:42	1.8	16	5408.3	1	4.33	QUENCH #16; #6 IN SUPERFLUID 16 A/S
QB023	22-Sep-96	22:39:03	1.8	16	6127.3	1	4.39	16 A/SEC QUENCH AT SUPERFLUID (1.8K) 17TH QUENCH OVERALL;
QB024	23-Sep-96	7:23:56	1.8	16	5897.4	6	3.83	"18TH QUENCH, 1.8K, 16A/SEC"
QB025	23-Sep-96	9:24:17	1.8	16	6200.7	1	4.83	"1.8K, 16A/SEC, 18TH QUENCH"
QB026	23-Sep-96	13:26:29	1.8	16	6083.3	1	4.72	"QUENCH #19 OVERALL, 1.8K, 16A/SEC"
QB027	23-Sep-96	15:10:34	1.8	16	5696.9	3	3.83	"QUENCH #20 (#10 AT 1.8K), 16A/S"
QB028	23-Sep-96	16:22:57	1.8	16	4933.8	2	3.78	"PREVIOUS RUN WAS A QDC#6 TRIP. THIS WAS A REDO - RAMP TO QUENCH AT 16A/S, 1.8K; AT AROUND 4KA QDC#2 TRIPPED..."
QB029	23-Sep-96	17:13:25	1.8	16	4977.8	2	3.86	"ANOTHER QDC#2 TRIP DURING RAMP AT 16A/S, 1.8K"
QB030	23-Sep-96	18:34:45	1.8	16	6264.3	1	4.71	"1.8K, 16A/SEC, QUENCH #20"
QB031	23-Sep-96	20:34:02	1.8	300	5158.8	1	4.08	"1.8K, 300A/SEC, 21ST QUENCH"
QB032	23-Sep-96	21:31:11	1.8	200	6005.0	1	4.32	"1.8K, 200A/SEC, 22ND QUENCH"
QB033	23-Sep-96	22:54:47	1.8	150	5995.3	1	4.51	"150A/SEC, 1.8K, 23RD QUENCH"
QB034	24-Sep-96	6:32:40	1.8	100	6137.1	1	4.10	"RAMP TO QUENCH ~ 100A/S, 1.8K, QUENCH #24 (#14 AT 1.8K)"
QB035	24-Sep-96	8:33:34	1.8		6220.3	1	4.09	"RAMP TO QUENCH AT A/S, QUENCH # 25 (#15 AT 1.8K)"
QB036	24-Sep-96	10:20:09	1.8	50	6293.6	1	4.30	QUENCH #26 OVERALL; 50A/SEC IN 1.8K HE II
QB038	24-Sep-96	14:05:19	1.8		1495.2	1	0.44	"HFU STUDY, 1.8K, 1500A, 295V"
QB039	24-Sep-96	14:16:21	1.8		1495.2	1	0.43	"HFU STUDY, 1.8K, 1500A, 318V"
QB040	24-Sep-96	14:23:28	1.8		1495.2	1	0.42	"HFU STUDY, 1.8K, 1500A, 339V"
QB041	24-Sep-96	14:30:30	1.8		1495.2	1	0.42	"HFU STUDY, 1.8K, 1500A, 360V"
QB042	24-Sep-96	14:37:46	1.8		1495.2	1	0.43	"HFU STUDY, 1.8K, 1500A, 379V"
QB043	24-Sep-96	14:58:00	1.8		2996.8	1	2.05	"HFU STUDY, 1.8K, 3000A, 200V"
QB044	24-Sep-96	15:16:00	1.8		2992.0	1	2.09	"HFU STUDY, 1.8K, 3000A, 191-197V"
QB045	24-Sep-96	15:27:19	1.8		2992.0	2	2.02	"HFU STUDY, 1.8K, 3000A,241V"
QB046	24-Sep-96	15:51:25	1.8		5188.2	1	4.32	"HFU STUDY, 1.8K, 5200A, 100-110V"
QB047	25-Sep-96	8:04:00	1.8	16	6269.2	1	4.58	"QUENCH AT 1.8K, 16A/SEC FOLLOWING 'FLOATING' OVER NIGHT"
QB048	25-Sep-96	9:55:46	1.8	16	6107.8	1	5.04	"RAMP TO QUENCH AT 16A/S, 1.8K; WAS SUPPOSED TO BE RAMP TO 6100A FOR HEATER STUDY"
QB050	25-Sep-96	13:27:25	1.8		5990.4	1	2.73	"6000A, HFU=120V, 1.8K HEATER STUDY"
QB051	25-Sep-96	14:55:16	1.8		5990.4	1	2.78	"147V HFU, 6000A, 1.8K"
QB052	25-Sep-96	16:18:03	1.8		5990.4	1	2.69	"HFU 190V, 6000A, 1.8K"
QB053	25-Sep-96	17:57:06	1.8		5990.4	1	2.65	HEATER QUENCH ATT 6000 A. HEATER VOLTAGE = 225V
QB054	25-Sep-96	19:21:31	1.8		5990.4	1	2.63	6000A HEATER TEST; 1.8K SHFU=252 V
QB055	25-Sep-96	20:49:32	1.8		5188.2	1	2.40	"5200A HEATER TEST, 1.8K, SHFU = 291 V"
QB056	25-Sep-96	21:45:14	1.8		5188.2	1	2.48	"HEATER STUDY 5200A, 1.8K, SHFU=191V"
QB057	25-Sep-96	22:47:02	1.8		6190.9	1	2.66	"HEATER TEST AT 6200A, 1.8K, SHFU=86V"
QB058	26-Sep-96	7:13:19	1.8	16	4801.8	1	3.34	"4.3K, 29TH QUENCH RETURN FROM 1.8K QUENCHES"
QB059	26-Sep-96	15:18:28	4.3		996.3	1	0.29	STRIP HEATER INDUCED QUENCH @1000AMPS. HTF 237V. DUMP DELAY .02SEC. T=4.3K.

File	Date	Time	Nom. Temp	Ramp Rate	Current	Q D C	MIITs	Comments
QB060	26-Sep-96	15:32:53	4.3		996.3	1	0.13	"4.3K HEATER STUDY; 1000A, SHFU=290V"
QB061	26-Sep-96	15:40:32	4.3		1001.2	1	0.12	"4.3K HEATER STUDY, 1000A, SHFU=335V"
QB062	26-Sep-96	15:51:23	4.3		996.3	1	0.12	"4.3K HEATER STUDY, 1000A, SHFU = 376V"
QB063	26-Sep-96	16:06:52	4.3		2297.4	1	0.78	"4.3K HEATER STUDY, 2300A, SHFU=201V"
QB064	26-Sep-96	16:31:18	4.3		3794.1	1	1.64	"4.3K HEATER STUDY, 3800A, 125V"
QB065	26-Sep-96	17:24:40	4.3		4493.6	1	2.02	"4.3K HEATER TEST, 4500A, SHFU=100V"
QB066	26-Sep-96	18:38:29	4.3		4493.6	1	1.84	"HEATER STUDY AT 4.3K, 4500A, SHFU=141V"
QB067	26-Sep-96	20:47:10	4.3		4493.6	1	1.78	"HEATER STUDY, 4500V, 173V, 4.3K"
QB068	26-Sep-96	21:29:10	4.3		4493.6	2	1.55	"HEATTER STUDY, 4.3K, 4500A, 223V"
QB069	26-Sep-96	22:50:10	4.3		4488.7	2	1.60	"HFU STUDY, 4500A, 283V, 4.3K"
QB070	27-Sep-96	7:26:49	3.6	16	5119.7	1	3.58	"3.6K, 16A/SEC, SPONTENAOUS QUENCH #30"
QB071	27-Sep-96	9:05:49	3.1	16	5369.2	1	3.91	"QUENCH #31 - 3.1K, 16A/SEC PART OF TEMP SCAN"
QB073	27-Sep-96	11:05:17	2.7	16	5515.9	1	4.06	"QUENCH #32, AT 2.7K, 16A/S"
QB074	27-Sep-96	14:22:23	2.15	16	5701.8	1	4.19	"QUENCH #33, AT 2.15K, 16A/S"
QB075	27-Sep-96	15:29:19	4.3		492.5	3		QDC#3 TRIP - LEAD FLOW NOT SET
QB076	27-Sep-96	17:22:22	4.3		3500.7	2	2.01	TRIP ON QDC#2 (MAGNET-IDOT) DURING FLATTOP
								AT 3500A FOR SPLICE MEASUREMENTS
QB077	27-Sep-96	18:14:33	4.3		3001.7	2		ANOTHER QDC#2 TRIP ...3000A FLATTOP DURING SPLICE MEASUREMENT
QB078	9-Oct-96	8:25:05	1.8		986.5	2	0.17	"1.8K, 1000A MANUAL TRIPP TO VERIFY SETTINGS"
QB079	9-Oct-96	8:59:27	1.8	16	5990.4	1	4.21	"1.8K, 1ST QUENCH TC2, DURING SG RUN, (QUENCH #34 OVERALL)"
QB080	9-Oct-96	10:56:06	1.8	16	6269.2	1	4.19	1.8K - 2ND AFTER THERMAL CYCLE
QB081	9-Oct-96	13:06:49	1.8	16	6093.1	1	4.64	"1.8K, 16A/SEC, 2ND THERMAL CYCLE, QUENCH #36"
QB083	10-Oct-96	7:47:28	1.8		1485.4	1	0.27	"1.8K, 1500A HEATER INDUCED QUENCH, SHFU=400V"
QB084	10-Oct-96	8:28:57	4.3		5902.3	1	3.15	QUENCH DURING RAMP TO 6000A FOR HEATER STUDY TEST
QB085	10-Oct-96	10:34:31	1.8		5990.4	1	2.64	"STRIP HEATER INDUCED QUENCH, 6000A, SHFU=338V, DURING STRAIN GAUGE RUN at 1.8K"
QB086	10-Oct-96	14:23:52	1.95	16	6058.8	1	3.23	"QUENCH AT 1.95K, 16 A/S, DURING A SG RUN"
QB087	10-Oct-96	16:24:21	3.8	200	3813.7	1		QUENCHED DURING 200 A/SEC AC LOSS MEASUREMENT @3.8K.
QB088	10-Oct-96	17:15:53	3.8	16	5095.2	1	2.55	"3.8K, 16A/SEC, SPONTENAOUS QUENCH"
QB089	10-Oct-96	17:57:32	3.8		986.5	1	0.13	1000 A VHFU 400V AT 4.3K
QB090	10-Oct-96	18:34:01	4.3		1236.0	1	0.36	"VH 232 VOLTS, T = 4.3 K I = 1250 A - V MIN STUDY"
QB091	10-Oct-96	19:34:00	4.3		1886.5	1	0.46	"I=1900,VHFU=225,4.3K"
QB092	10-Oct-96	19:47:00	4.3		4488.7	2	1.65	4500 A 400 V VHU 4.3 K
QB093	10-Oct-96	20:38:32	4.3		4855.6	1	2.26	RAMP TO QUENCH AT 4.3K AND 23 PSI
QB094	10-Oct-96	22:13:19	4.3		986.5	1	0.27	1000A 4.3 K 1.5 ATM VHFU 230 V
QB095	10-Oct-96	22:32:45	4.3		1485.4	1	0.43	"VMIN STUDY CONTINUES VHFU=220, I=1500 4.3K 1.5ATM"
QB096	10-Oct-96	23:03:00	4.3		4488.7	1	2.03	"VMIN STUDY VHFU=105, I=4500,4.3K 1.5 ATM"